Chapter 3: Characterization of carbene complexes

The new complexes were characterized and studied by infrared and NMR spectroscopy, as well as by mass spectrometry. In dealing with metal carbonyl carbene complexes, valuable information can be obtained from the spectral features and band positions. NMR spectroscopy is invaluable in assigning structures to the complexes that were synthesized and the technique of IR spectroscopy confirms the presence and symmetry of metal carbonyls. Observing an M^+ ion in the mass spectrum is strong evidence that the complex was identified correctly.

3.1 Proton NMR spectroscopy data

3.1.1 Monocarbene dirhenium nonacarbonyl complexes

3.1.1.1 Thiophene precursors

The NMR chemical shifts (^1H, ^{13}C) for thiophene, bithiophene and 3,6–dimethylthieno[3,2–*b*]thiophene (carbene R–substituents) are shown in Figure 3.1.

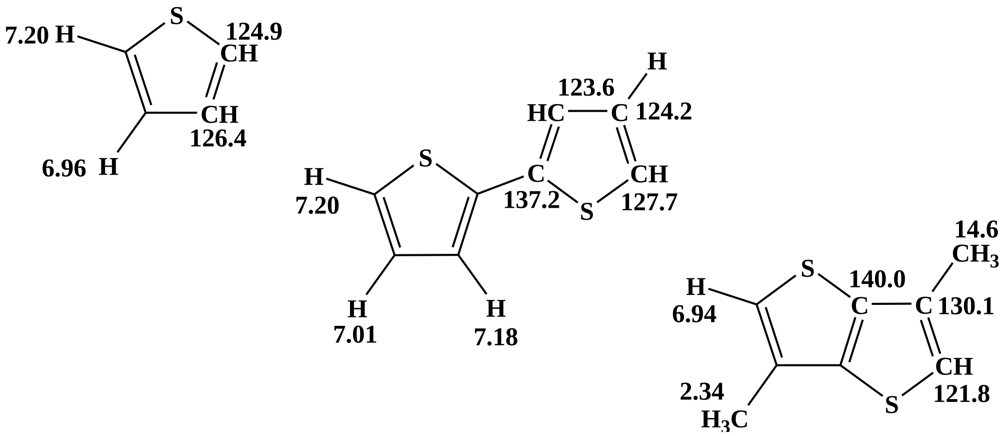

Figure 3.1: Chemical shifts (^1H; ^{13}C) NMR spectroscopy data (ppm) for thiophene and the thienyl substituents

3.1.1.2 Dirhenium complexes

The dirhenium monocarbene complexes **1** to **3** were prepared from the 2–lithiumthienyl precursors, as discussed in Chapter 2. The aromatic region of the ^{1}H NMR spectrum of complex **2** is shown in Figure 3.2. The spectrum was recorded in deuterated chloroform and the chloroform peak in the spectrum used for calibration (7.24 ppm).

There are two doublets – at 7.73 and 7.18 ppm – that belong to the hydrogen atoms on the thiophene ring to which the carbene is attached. The two hydrogen atoms couple and their signals are split into doublets. The signal at 7.73 ppm is identified as belonging to ring hydrogen H3, because it is shifted furthest downfield by the adjacent electrophilic carbene carbon atom (0.72 ppm, Table 3.1), whilst the signal of H4 is not shifted at all from its position in the ^{1}H NMR spectrum of bithiophene. The highest field signal belongs to H8 and it lies at 7.05 ppm. This signal is shifted slightly downfield from its position in the spectrum of bithiophene. It is split because H8 couples to the two neighbouring hydrogen atoms, H7 and H9. The signal does not appear as a doublet of doublets, but as a triplet with satellite signals each side of the middle peak of the signal. Interestingly, the signal of the ring proton (H9) that is the farthest from the electron–drawing carbene carbon is shifted more downfield than that of H8. The sum of the integration values of the peaks give a value of 4.82, close enough to 5 to be indicative of five protons.

There are two unidentified small doublet signals at 7.93 and 7.25 ppm. These signals are presumed to go together and belong to a symmetrical complex or molecule. The species could not be identified, but it is not 5,5′–diformyl–2,2′–bithiophene.

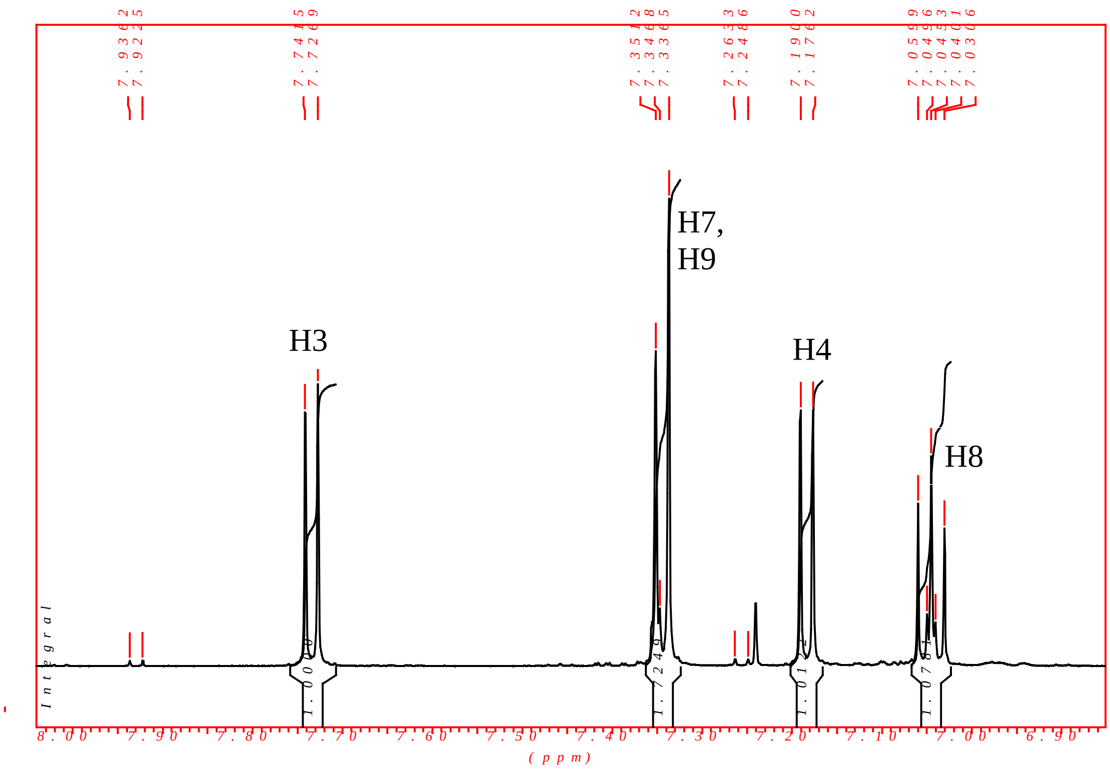

Figure 3.2: Aromatic region of the ^{1}H NMR spectrum of **2** in $CDCl_3$

The ^{1}H NMR data for the three monocarbene complexes are given in Table 3.1.

The electron–withdrawing carbene carbon is directly attached to a thienyl ring. The molecular configuration can be compared to other aromatic ring systems that have electron–withdrawing groups. For thiophene, there are a multitude of examples that have been synthesized, from thiophene rings with carboxylic groups at the α–position to halides, metals and other thienyl rings[1]. There are not as many examples for bithiophene and 3,6–dimethylthieno[3,2–*b*]thiophene. 2–Thiophenecarboxylate[2] is an organic analogue of the thiophene monocarbene complex **1**. Its ring protons have signals at 7.80 (H3), 7.10 (H4) and 7.55 ppm (H5) in CD_2Cl_2. The same signal pattern is observed in the aromatic region of the thiophene complex **1**.

---

[1] (a) S. P. Ivonin, A. A. Tolmachev, A. M. Pinchuk; *Curr. Org. Chem.*, **2008**, *12*, 25–38; (b) W–Y. Wong, K–H. Choi, G–L. Lu; *Organometallics*, **2002**, *21*, 4475–4481

[2] H. Satonaka; *Bull. Chem. Soc. Jpn.*, **1983**, *56*, 2463–2468

Table 3.1: ^{1}H NMR spectral data (δ, J (Hz), CDCl$_3$) of **1**–**3**

$\Delta\delta_R$ = difference from free substituent; value in ppm			
Complexes:	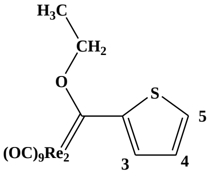 **1**	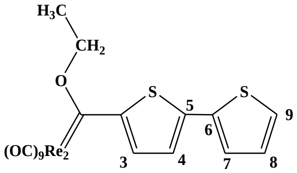 **2**	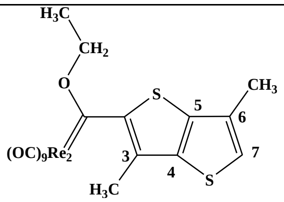 **3**
H3	7.65 (d, 4.4)[a] $\Delta\delta_R$[b] = 0.69	7.73 (d, 4.6) $\Delta\delta_R$ = 0.72	–
Me3	–		2.16 (s) $\Delta\delta_R$ = –0.18
H4	7.11 (t, 4.4; 4.7) $\Delta\delta_R$ = 0.15	7.18 (d, 4.6) $\Delta\delta_R$ = 0.00	–
H5	7.65 (d, 4.7) $\Delta\delta_R$ = 0.45	–	
H7	–	7.35 (d, 4.6) $\Delta\delta_R$ = 0.17	7.04 (q, 1.0) $\Delta\delta_R$ = 0.10
H8	–	7.05 (dd, 1.3, 4.6) $\Delta\delta_R$ = 0.04	–
Me6	–		2.39 (d, 1.0) $\Delta\delta_R$ = 0.05
H9	–	7.35 (d, 4.4) $\Delta\delta_R$ = 0.15	–
OC**H$_2$**CH$_3$	4.51 (q, 7.0)	4.54 (q, 7.0)	4.40 (q, 7.0)
OCH$_2$C**H$_3$**	1.58 (t, 7.0)	1.60 (t, 7.0)	1.50 (t, 7.0)

[a] (J in Hz)

[b] $\Delta\delta_R$ = difference between the chemical shifts of the corresponding protons of the thiophene substrates and the thienyl substituent of the complexes

The protons of the aromatic substituent in complexes **1** and **2** that are closest to the carbene carbon atom are the H3 protons. Their signals are shifted downfield, which indicates that the carbene carbon atom has a deshielding effect on the thienyl ring. Overall the perception is that the ester carbon (2–thiophenecarboxylate) and the carbene carbon have a very similar electron–withdrawing effect on the thiophene ring.

The change in chemical shift of H3′s signal in complex **2** (versus the same hydrogen in bithiophene) is about the same as the signal–shift of proton H3 of complex **1**. In complex **1** H3′s signal is shifted 0.69 ppm downfield (6.96→7.65 ppm) and in the bithiophene monocarbene complex **2**, it is shifted downfield by 0.72 ppm (7.01→7.73 ppm). On the other hand, the signal of H4 of complex **1** is shifted downfield ($\Delta\delta_R$ = 0.15 ppm) whereas H4 of complex **2** is not shifted downfield at all ($\Delta\delta_R$ = 0.00 ppm).

The second ring of bithiophene complex **2** has three hydrogen atoms. Their signals are also shifted downfield by the attachment of the electrophilic carbene carbon in the 2 position. The signals of H7 and H9 are shifted the most and H8's signal is shifted downfield the least (respectively $\Delta\delta_R$ = 0.17, 0.15 and 0.04 ppm).

In the spectrum of complex **3**, it was unexpected to observe that the signal of the closest methyl, Me3, is shifted upfield instead of downfield. There are two probable signals for the thienyl methyls and the assignment was made by looking at the coupling. Me6 couples to H7 and its signal is split into a doublet whereas the signal of Me3 is a singlet.

The three monocarbene complexes have the following ring protons that are farthest from the carbene carbon atom: in **1** it is H5, in **2** it is H9 and in **3** H7. H5 of complex **1** is shifted downfield the most of these three complexes, as is expected. However, the H9 signal of complex **2** is shifted downfield more than the H7 signal of complex **3**.

It is interesting that in complex **1** the signals of the closest thiophene proton, H3, and of the farthest thiophene proton, H5, are at the same chemical shift value. The same is also seen for the second ring of the bithiophene monocarbene complex (H7 and H9 signals fall at the same shift value), as is indicated below.

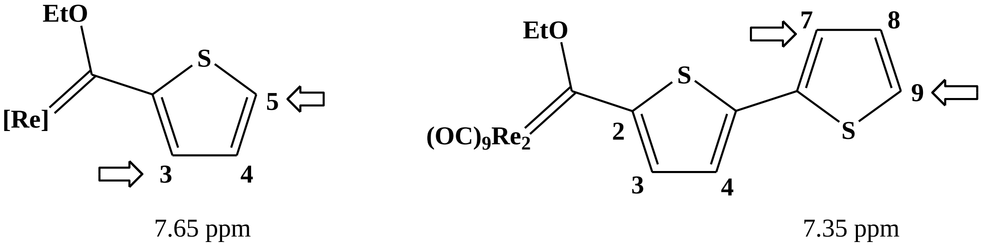

Figure 3.3: Ring hydrogen atoms that have coinciding signals in the ^{1}H NMR spectra

It can be shown with a calculation, that the electron–withdrawing property of the carbene carbon atom is transmitted to the second ring of **2** through the first. Consider the similarities of the two rings marked with asterisks in Figure 3.4.

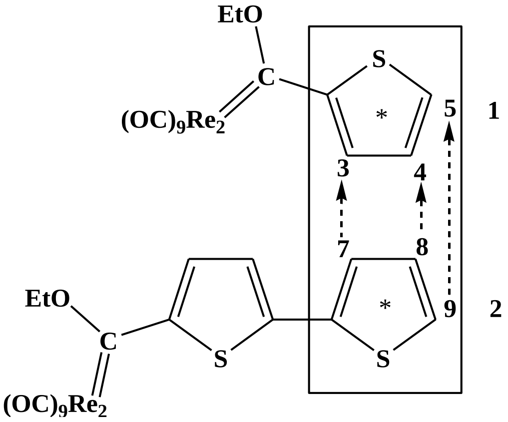

Figure 3.4: Correlation between ring hydrogen atoms of two different complexes

The electron–withdrawing power, exercised by the group at pseudo–position '2' on ring two in bithiophene complex **2**, is about ¼ to a $^1/_3$ of what is exercised on a thiophene ring that is directly attached to the carbene carbon atom, as given here:

(0.17 ppm/0.69 ppm = 0.25) (Δδ(H7) of **2** / Δδ(H3) of **1**)

(0.04 ppm/0.15 ppm = 0.27) (Δδ(H8) of **2** / Δδ(H4) of **1**)

(0.15 ppm/0.45 ppm = 0.33) (Δδ(H9) of **2** / Δδ(H5) of **1**)

Thiophene and the thienyl substituents have double bonds in conjugation. Resonance delocalization of these double bonds directly affects the distribution of electron density in the molecules. Thus it plays an important role in the NMR shifts that one observes for these complexes. In Scheme 3.1 the resonance delocalization of the three monocarbene complexes is illustrated. Even the farthest double bond can be involved in the stabilization of the carbene carbon. The resonance structures of Scheme 3.1 show how double bond delocalization produces partial positive charges on certain carbon atoms. The C1 carbon is the carbene carbon. The delocalization of bond C2–C3 to C1–C2 would for instance place a partial positive charge on ring carbon atom 3.

The greatest signal shifts observed are those of H3 (in complexes **1** and **2**) and so the delocalization is taken to be greatest for the C2–C3 (first) double bond. The bithiophene complex has more double bonds available that can be brought into conjugation than the thiophene or 3,6–dimethylthieno[3,2–*b*]thiophene complexes. The transfer of electron density from the distant thiophene ring in bithiophene is not so great, but still relevant. The same is true for H7 of the 3,6–dimethylthieno[3,2–*b*]thiophene substituent in complex **3**. Therefore the chemical shifts confirm that the farther away, the less involvement there is in carbene stabilization by ring electron delocalization, even though the ligands are flat and π–conjugation is possible.

Besides local π–effects there is a general loss of electron density from the electron–excessive thienyl rings towards the carbene carbon atom.

At room temperature the two CH_2 hydrogen atoms of the ethoxy substituent are equivalent and so are the three CH_3 hydrogen atoms. Their signals are observed as, respectively, a quartet and a triplet in the ^1H NMR spectra of the three complexes because the CH_2 and CH_3 protons couple.

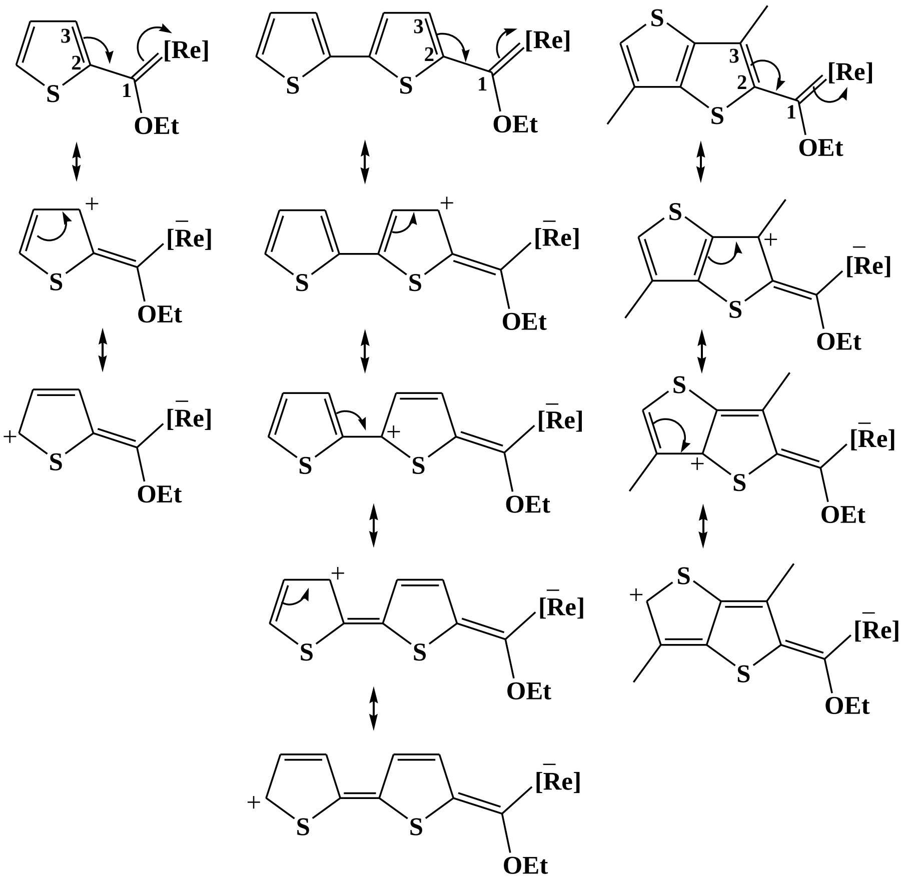

Scheme 3.1: Double bond delocalization in thienyl substituents

The above conclusions can also be illustrated by a simple calculation that can be done for each individual ring hydrogen atom of a complex to determine the percentage of shift of the ring protons relative to the shift of the proton that has the largest shift (100%). The outcome supports the conjugation explanation for deshielding of ring hydrogen atoms:

1: **H3** (100%), H5 (65%) and H4 (22%)
2: **H3** (100%), H7 (24%), H9 (21%), H8 (6%), H4 (0%)

The data of the biscarbene complexes **7**–**9** are discussed next, as they have similar shifts on the ^{1}H NMR spectrum than the monocarbene complexes **1**–**3**. The bromine–cleaved complexes (**4**–**6**) will be discussed in section 3.1.3.

3.1.2 Biscarbene tetrarhenium complexes

The biscarbene complexes (**7**–**9**) were prepared by reacting [$Re_2(CO)_{10}$] with dilithiated thiophene substrates. The biscarbene complexes **7** and **9** proved elusive, forming in low yield and reacting on the column with trace amounts of water. The bithiophene biscarbene complex **8** formed in higher yield and reacted slower on the silica gel column. Proton NMR spectra were measured for these complexes (Table 3.2).

The aromatic to CH_2 (of the ethoxy substituent) region of the ^1H NMR spectrum of complex **8** is shown in Figure 3.5. The spectrum was recorded in deuterated chloroform and the chloroform peak was used for calibration. A singlet at 5.28 ppm belongs to residual dichloromethane. Integration values show that the two aromatic signals in the spectrum belong to the same number of hydrogen atoms – it is known that each signal corresponds to two hydrogen atoms. The integration value (2.23) for the four equivalent CH_2 (of OCH_2CH_3) protons is slightly high, but still acceptable and indicates a 1:2 ratio between outer, or inner, ring hydrogen atoms and CH_2 hydrogen atoms.

The two outer hydrogen atoms and the two inner hydrogen atoms of the bridging bithiophene are equivalent, because the molecule has a symmetry centre. Thus there are only two signals for the four ring protons. The protons on each ring couple with each other and their signals are split into doublets. At 7.30 ppm, the H4 and H4' signals appear close to where the signals of H7 and H9 of complex **2** were found. The H4 signal of complex **2** appears at higher field strength, though.

The signal of the CH_2 protons of the ethoxy carbene substituent is split into the expected quartet by the CH_3 protons of the ethoxy substituent. The quartet location at 4.51 ppm shows again how the electronegative oxygen atom, under the influence of the carbene carbon atom, deshields the attached CH_2 protons.

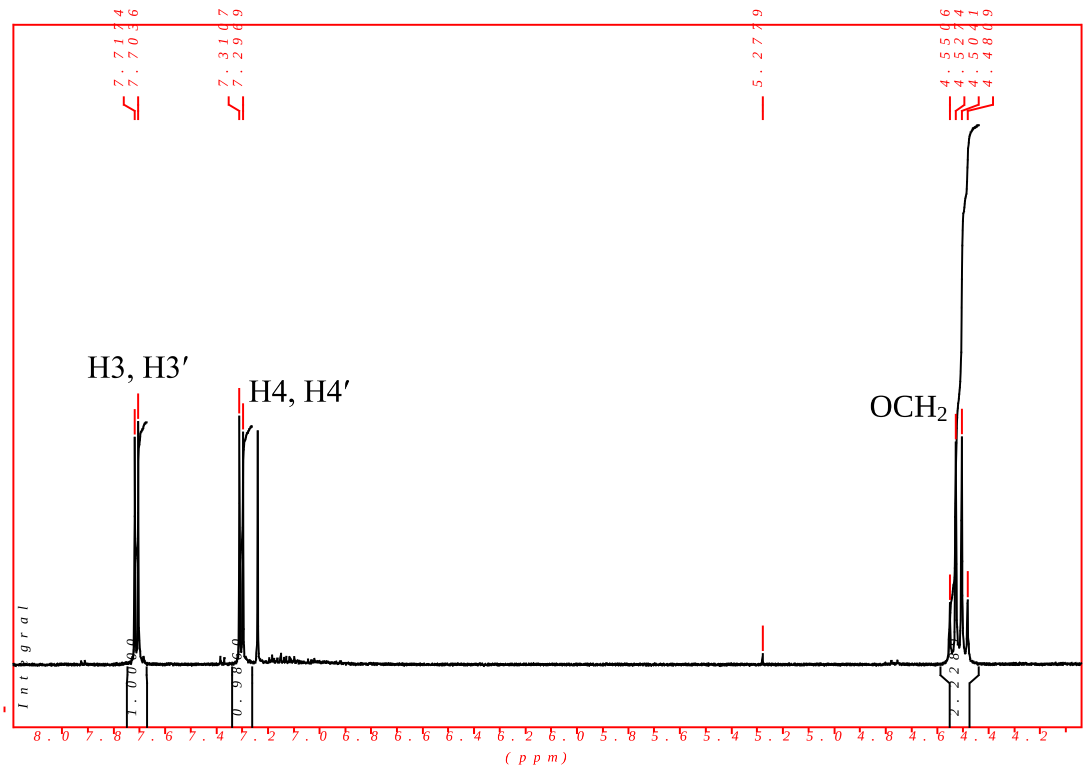

Figure 3.5: A part of the ^{1}H NMR spectrum of complex **8** in $CDCl_3$

The ^{1}H NMR data of thiophene biscarbene complex **7** displays a signal for the two ring proton that appear upfield from the H3 position in the spectrum of monocarbene complex **1**. It may be that resonance delocalization is reduced in this complex, possibly due to a larger twist between the thiophene plane and the carbene planes. The CH_2 signal of the ethoxy substituents is also found upfield from its position in complex **1**, so there is less electron–density donation from this carbene substituent to the carbene carbon atom.

The H3/H3' signals of biscarbene complex **8** are very close to those of H3 of monocarbene complex **2**. According to the data, H4 of complex **8** is more deshielded than H7 of complex **2**. The carbene attached to the other thiophene ring can produce a partial positive charge on C4 through resonance delocalization. With respect to this carbene H4 is in the same location as H7 is with respect to the carbene in the monocarbene complex. There is, in this complex, the combined effect of two electron withdrawing carbene carbon atoms, compared to one in **2**, and there should generally be less electron density on the thiophene rings.

Table 3.2: ^{1}H NMR spectral data (δ, J (Hz), $CDCl_3$) of **7**–**9**

Complexes:	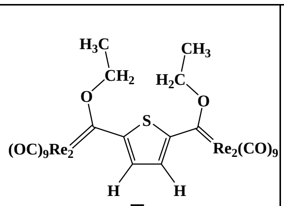 **7**	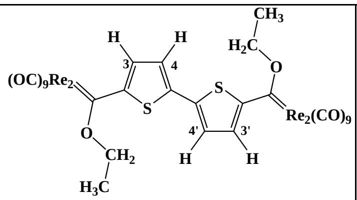 **8**	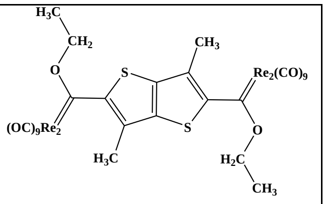 **9**
H3	7.47 (s) $\Delta\delta_R = 0.67$	7.71 (d, 4.1) $\Delta\delta_R = 0.70$	–
H4	–	7.30 (d, 4.1) $\Delta\delta_R = 0.12$	–
Me3	–		2.21 (s) $\Delta\delta_R = -0.13$
$OC\mathbf{H_2}CH_3$	4.42 (q, 7.0)	4.51 (q, 7.0)	4.41 (q, 7.0)
$OCH_2C\mathbf{H_3}$	1.57 (t, 7.0)	1.61 (t, 7.0)	1.54 (t, 7.0)

In complex **8** the most important resonance form is the one that depicts a deshielding of hydrogen atoms H3 and H3′. A resonance form that places partial positive charges on C5 and C5′ is not considered feasible (Scheme 3.2).

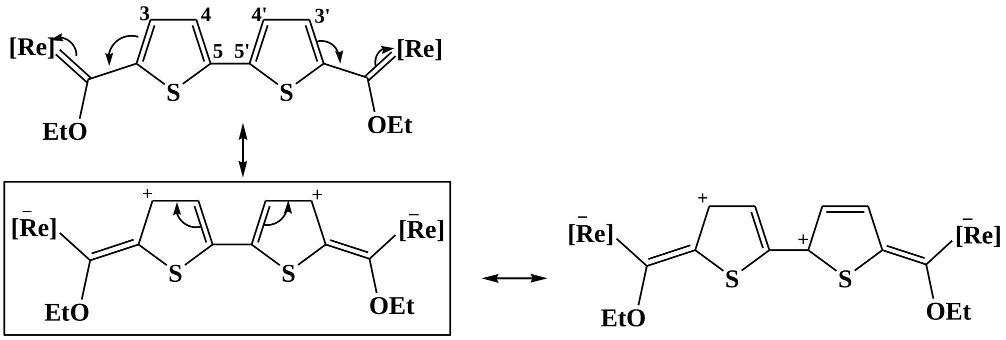

Scheme 3.2: Resonance forms for complex **8**

For complex **9** there are no signals in the aromatic region as the four ring carbon atoms have either a methyl or a carbene fragment as external group. Because the complex is symmetrical, only one signal is observed for the two methyls. Recalling that the ^{1}H NMR values for the pendant methyl groups of monocarbene complex **3** are 2.16 (Me3) and 2.39 ppm (Me6), it is interesting to find a value for complex **6** (2.21 ppm) that lies between these two values. With the ^{1}H NMR shift of the methyl groups of the free substituent being 2.34 ppm, one also again observes an odd upfield shift of the signal.

3.1.3 Bromo monocarbene complexes of rhenium

The bromo monocarbene complexes (**4**–**6**) of rhenium were prepared by reacting dirhenium carbene complexes **1**–**3** with bromine. The structural difference between the cleaved and uncleaved complexes is X in [Re(CO)$_4${C(OEt)thienyl}X], with X either being “Re(CO)$_5$” or “Br”.

In Figure 3.6, a section of the proton NMR spectrum of complex **5** is shown. The ^{1}H NMR spectrum was recorded in deuterated chloroform and the chloroform signal at 7.24 ppm used for calibration. This complex is a bithiophene monocarbene complex similar to complex **2** and the same signal pattern is observed as that seen for complex **2**. It is evident that the signals of the aromatic ring protons of these complexes are shifted downfield if the rheniumpentacarbonyl fragment is replaced by a bromo ligand. H3′s signal, specifically, is shifted downfield drastically. The signal of this proton is split into a doublet by coupling to the other hydrogen atom of the thiophene ring and there is also a small doublet that may indicate another isomer.

The H7 and H9 signals almost overlap, as for complex **2**. Their signals are not much shifted downfield from their position in the uncleaved complex. The signal of H8 is split into a doublet of doublets, as it couples with H7 and H9. The signals of these protons are split into doublets of doublets, indicating that they also couple with each other.

The quartet signal of the CH_2 protons is also shifted downfield. The signal overlaps with that of dichloromethane.

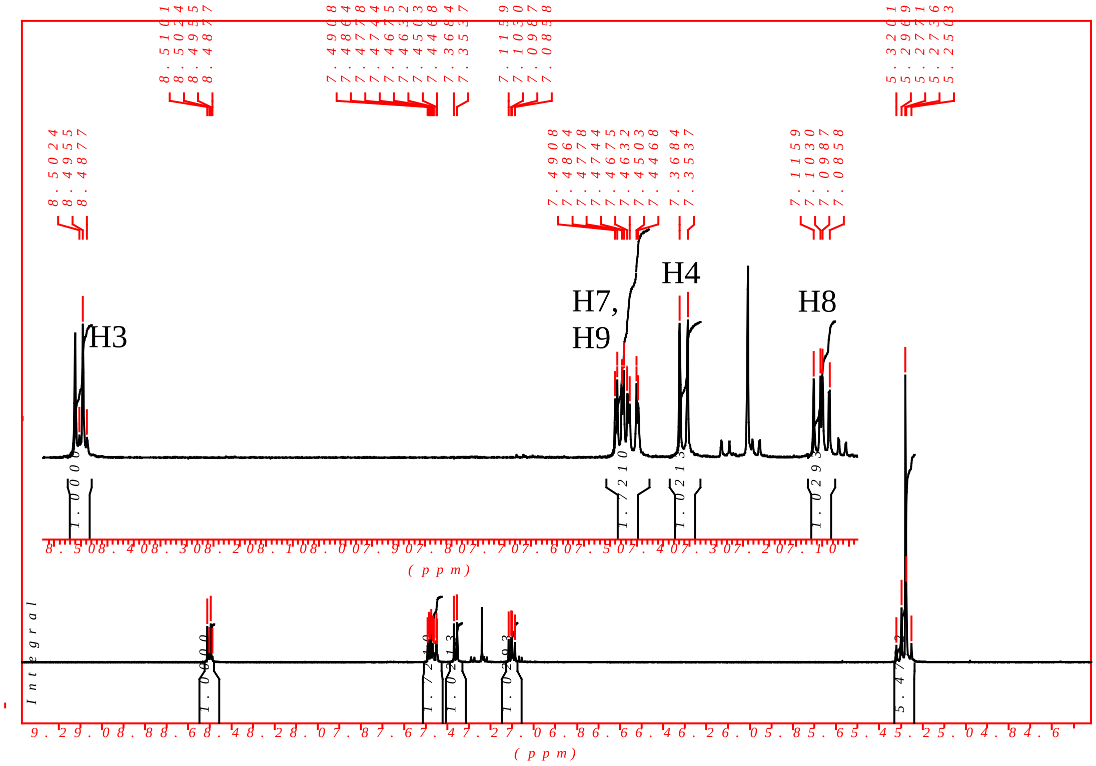

Figure 3.6: ^{1}H NMR spectrum of complex **5** in $CDCl_3$

The data for the three cleaved monocarbene complexes are given in Table 3.3.

As with the uncleaved complexes, the ring hydrogen atoms are affected by the electrophilic carbene carbon atom. Their shifts are even more downfield, compared to the free substituents. For a bromo ligand, less electron density is placed on the metal, which is back bonded to the π–acceptor ligands. Thus, a greater demand for electron density is transferred to the thienyl substituent by the electrophilic carbene carbon atom.

Table 3.3: ^{1}H NMR spectral data (δ, J (Hz), $CDCl_3$) for **4**–**6**

Complexes:	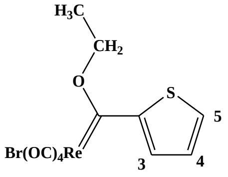 **4**	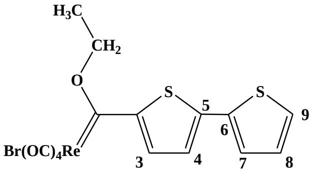 **5**	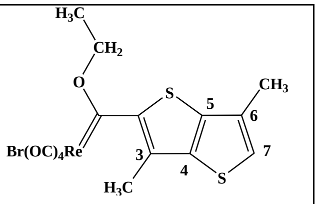 **6**
H3	7.98 (dd, 4.9; 1.0) $\Delta\delta_R = 1.02$; $\Delta\delta_U{}^{a} = 0.33$	8.50 (d, 4.4) $\Delta\delta_R = 1.49$; $\Delta\delta_U = 0.77$	–
Me3	–		2.56 (s) $\Delta\delta_R = 0.22$; $\Delta\delta_U = 0.17$
H4	7.19 (dd, 4.5; 4.2) $\Delta\delta_R = 0.23$; $\Delta\delta_U = 0.08$	7.36 (d, 4.4) $\Delta\delta_R = 0.18$; $\Delta\delta_U = 0.18$	–
H5	7.79 (dd, 4.5; 1.0) $\Delta\delta_R = 0.59$; $\Delta\delta_U = 0.14$	–	
H7	–	7.48 (dd, 3.6; 1.0) $\Delta\delta_R = 0.30$; $\Delta\delta_U = 0.08$	7.50 (s) $\Delta\delta_R = 0.56$; $\Delta\delta_U = 0.46$
H8	–	7.09 (dd, 3.6; 5.2) $\Delta\delta_R = 0.08$; $\Delta\delta_U = 0.04$	–
Me6	–		2.42 (d, 1.3) $\Delta\delta_R = 0.07$; $\Delta\delta_U = 0.26$
H9	–	7.45 (dd, 5.2; 1.0) $\Delta\delta_R = 0.25$; $\Delta\delta_U = 0.11$	–
$OC\mathbf{H_2}CH_3$	4.78 (q, 7.0) $\Delta\delta_U = 0.27$	5.28 (q, 7.0) $\Delta\delta_U = 0.74$	5.57 (q, 7.0) $\Delta\delta_U = 1.17$
$OCH_2C\mathbf{H_3}$	1.68 (t, 7.0) $\Delta\delta_U = 0.10$	1.66 (t, 7.0) $\Delta\delta_U = 0.06$	1.69 (t, 7.0) $\Delta\delta_U = 0.19$

[a] $\Delta\delta_U$ = difference between the chemical shifts of the corresponding protons of the thienyl substituent of the Br–cleaved and the uncleaved complexes

If one were to specifically consider ring proton H3 of complex **4**, it can be seen (as depicted in Figure 3.7), that a rigid six–membered ring will place H3 close to the more electronegative bromide ligand. Electronic interaction of Br with H3 will deshield the nucleus of H3 (see solid state structure of complex **5** in Chapter 4), leading to its signal being significantly shifted downfield in the ^{1}H NMR spectrum.

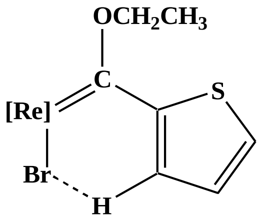

Figure 3.7: Intramolecular hydrogen bonding between Br and H in **4**

Comparison shows that all the ring hydrogen atoms are not affected to the same extent by the carbene carbon. A calculation was done for **4** and **5** to determine which resonance forms carry the highest weight. Again the values relative to the proton farthest downfield is expressed as a percentage:

4: **H3** (100%), H5 (<u>58%</u>) and H4 (<u>23%</u>)
5: **H3** (100%), H7 (<u>20%</u>), H9 (<u>17%</u>), H4 (<u>12%</u>), H8 (<u>5%</u>)

These values act as verification of the influence of double bond delocalization to produce partial positive charges on certain ring carbon atoms. In the thiophene monocarbene complex **4**, the ring proton with the largest shift, due to bromide replacement of "$Re(CO)_5$", is H3. In complex **1** there seems to be a slightly greater contribution to stabilization from H5 (which indicates C4–C5 delocalization), than in the cleaved thiophene complex **4** (it was 65% in the case of **1**).

The same trend is observed when one compares bithiophene uncleaved and cleaved complexes **2** and **5**. In fact, the signal of H3 is dramatically shifted downfield, possibly pointing to a significant interaction between the bromo ligand and this hydrogen atom.

The second ring of the bithiophene complex is little affected by the ligand change on the metal. One notes that H9′s NMR signal is more downfield–shifted than that of H7, although it lies farthest away from the carbene.

In complex **6**, the resonance form that places a partial positive charge at position 3 of the ring may be the dominating resonance form (as is the case for the thiophene and bithiophene complexes). The Me6 signal is shifted downfield even more than that of Me3 (as compared to the free substituent), whereas its signal was seen to be shifted upfield in **3**. A downfield shift is a more intuitive adjustment. The signal of Me6 is a doublet because it couples with H7. The signal of H7 was observed to be a quartet, as expected.

The relocation of electron density from the aromatic substituents to the carbene carbon has the effect of the ring hydrogen NMR signals being shifted downfield (because they are partially deshielded). The difference between the corresponding ring hydrogen NMR values of the uncleaved and the cleaved complexes, allows for certain structure predictions.

A complex is proposed and shown in Figure 3.8. In the complex the ring has lost its aromatic character. A full positive charge is located on C3, and it would be expected that in this complex, the ^{1}H NMR signal of H3 would be shifted downfield substantially.

The carbene and aromatic substituent planes in **4** are not coplanar (see Chapter 4 for crystal structure and discussion) and therefore it is not expected that the proposed complex would be obtained by complete delocalization of the electron density in the C2–C3 double bond of **4**, to C1–C2. However, a more downfield–shifted H3 signal might point to a smaller angle between the carbene plane and the substituent plane. Crystal data have shown that indeed, for the cleaved complexes the possibilities of conjugation are greater because the angles between the planes are in fact smaller.

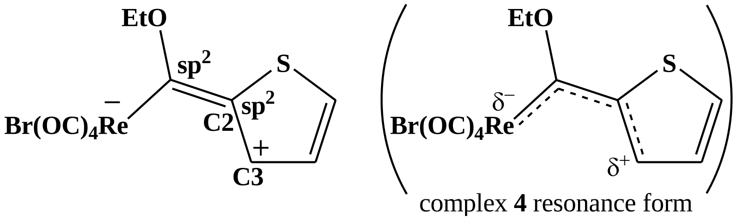

Figure 3.8: Double bond delocalization of **4**

There are significant changes in the value of the “CH_2” protons of the ethoxy substituent upon reaction with Br_2, but as expected, not in the values of the distant “CH_3” protons.

It is expected that, of the three complexes, the carbene π–stabilization from the rhenium in **4** should be the largest, since both the thiophene substituent and the ethoxy group hydrogen atom signals are not shifted downfield as dramatically. In **5**, the ^{1}H NMR data provides one with a sense that more contribution comes from the thienyl substituent to alleviate the electron shortage on the carbene carbon atom than that which is provided by the thienyl substituent in **6**. The ethoxy group in turn contributes more in **6** (the “CH_2” signal is shifted downfield the furthest).

3.1.4 Biscarbene bromo–carbene complexes

The cleavage of the rhenium–rhenium bonds of the biscarbene tetrarhenium bithiophene complex **8** was studied and products associated with a stepwise rhenium–rhenium cleavage could be isolated. Biscarbene complex **8** was reacted with one equivalent of Br_2(l) to produce **10** (major product) and **11** (minor product). It is interesting that one equivalent of Br_2(l) already produced mostly the bis–cleaved complex. Proton NMR data is given in Table 3.4.

Complex **10** displays a similar shift in the H3 signal (versus the uncleaved biscarbene complex and free bithiophene) as was seen in the case of monocarbene bromo complex **5**. The ethoxy group “CH_2” protons are slightly more deshielded in **10** than in the precursor **8**, relative to what was seen on going from **2** to **5** (monocarbene complexes). It also shows a greater involvement of the ethoxy groups in the carbene stabilization of the bromo–carbene complexes than in the $Re(CO)_5$–carbene complexes.

Table 3.4: ^1H NMR data (δ, J (Hz), $CDCl_3$) of bithiophene complexes **10** and **11**

Complexes:	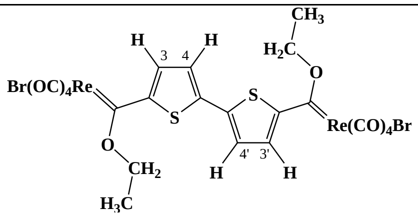 **10**	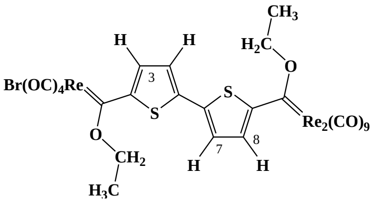 **11**
H3	8.56 (d, 4.4) $\Delta\delta_R = 1.55$; $\Delta\delta_U = 0.85$	8.52 (dd, 4.5) $\Delta\delta_R = 1.51$; $\Delta\delta_U = 0.81$
H4	7.58 (d, 4.7) $\Delta\delta_R = 0.40$; $\Delta\delta_U = 0.28$	7.43 (d, 4.6) $\Delta\delta_R = 0.25$; $\Delta\delta_U = 0.13$
H7	–	7.41 (d, 4.2) $\Delta\delta_R = 0.23$; $\Delta\delta_U = 0.11$
H8	–	7.73 (d, 4.2) $\Delta\delta_R = 0.72$; $\Delta\delta_U = 0.02$
$ReBr(CO)_5$: $OC\mathbf{H_2}CH_3$	5.35 (q, 7.0) $\Delta\delta_U = 0.94$	5.35 (q, 7.0) $\Delta\delta_U = 0.94$
$ReBr(CO)_5$: $OCH_2C\mathbf{H_3}$	1.66 (t, 7.0) $\Delta\delta_U = 0.05$	1.70 (t, 7.0) $\Delta\delta_U = 0.00$
$Re_2(CO)_9$: $OC\mathbf{H_2}CH_3$	–	4.41 (q, 7.0)
$Re_2(CO)_9$: $OCH_2C\mathbf{H_3}$	–	1.61 (t, 7.0) $\Delta\delta_U = 0.00$

Mixed–carbene complex **11** is perhaps a more interesting complex than complex **10** as **11** has two different metal fragments attached to the bithiophene. Two separate resonance sets can be described for the bithiophene biscarbene complex, because the carbene carbons have independent and competitive electron withdrawing effects on the adjacent thiophene ring protons. It is possible to compare the two attached metal fragments' electron–drawing ability. Because the ring hydrogen atom located closest to the $\{Re(CO)_4Br\}$ fragment has a resonance at 8.52 ppm, versus 7.73 ppm for the ring hydrogen atom closest to the $\{Re_2(CO)_9\}$ fragment, in Scheme 3.3 below, the upper resonance form is assumed to be more contributing. The bromo–carbene fragment has a stronger electron–withdrawing effect, compared to a $Re(CO)_5$–carbene fragment.

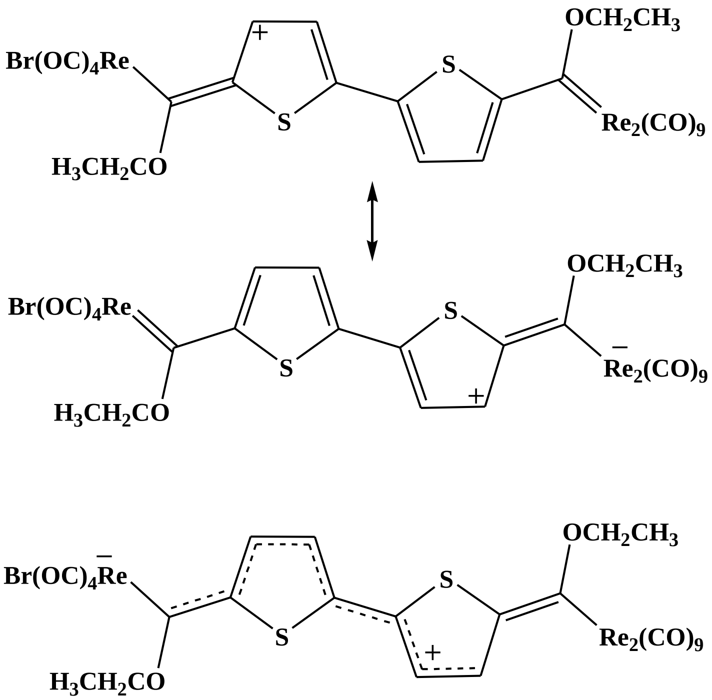

Scheme 3.3: Competing resonance forms for **11**

The differences between the outer ring hydrogen atoms of **11** (H3–H9 = 8.52 ppm–7.73 ppm = 0.79 ppm), are similar to the difference between the H3/H3′ hydrogen atoms of cleaved biscarbene complex **10** (8.56 ppm) and the uncleaved biscarbene complex **8** (7.71 ppm).

3.1.5 Carbene–aldehyde complexes

The reactive biscarbene tetrarhenium complexes were modified to carbene–aldehyde complexes. Based on spectroscopic data the conversion of metal–carbene units to aldehydes is postulated to commence via an intermediate that contains a hydroxycarbene ligand. The ^{1}H NMR data of the aldehyde complexes is given in Table 3.5.

Table 3.5: ^{1}H NMR data (δ, J (Hz), $CDCl_3$) for **12–14**

Complexes:	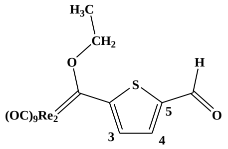 **12**	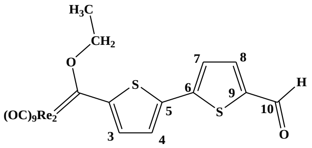 **13**	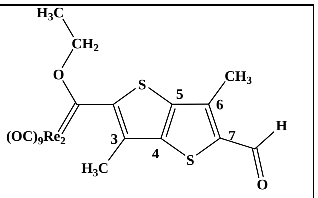 **14**
H3	7.82 (d, 4.1) $\Delta\delta_R = 0.86$	–	–
H4	7.72 (d, 4.1) $\Delta\delta_R = 0.76$	7.34 (d, 4.4) $\Delta\delta_R = 0.33$	
H5		–	
H7	–	7.23 (d, 4.1) $\Delta\delta_R = 0.05$	
H8	–	7.70 (d, 4.1) $\Delta\delta_R = 0.69$	
C(O)**H**	9.95 (s)	9.95 (s)	10.09 (s)
OC**H$_2$**CH$_3$	4.39 (q, 7.0)	4.42 (q, 7.0)	4.36 (q, 6.98)
OCH$_2$C**H$_3$**	1.72 (t, 7.0)	1.61 (t, 7.0)	1.51 (d, 6.99)
Me3 Me6	–	–	2.34 (s) 2.15 (s)

The aldehyde hydrogen of the carbene complexes shows a characteristic proton NMR signal at around 10 ppm. The ^{1}H NMR values of organic aldehydes are given below. It is believed that differences between the signal locations of 5–formyl–2,2'–bithiophene, isolated and characterized in this study, and reported 5–formyl–2,2'–bithiophene ^{1}H NMR spectroscopy values are due to different solvents having been used to determine the ^{1}H NMR spectra.

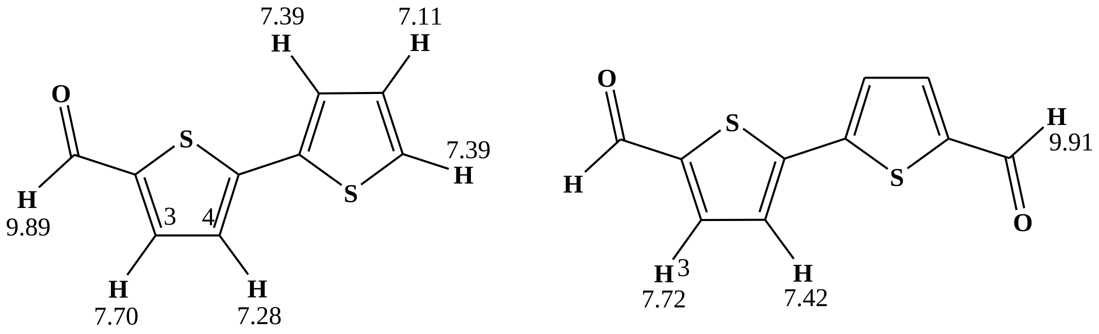

Figure 3.9: ^{1}H NMR data (ppm) for 5–formyl–2,2′–bithiophene[3] (acetone–d_6) and 5,5′–diformyl–2,2′–bithiophene[4] (chloroform–*d*)

Complex **12** presents an interesting case as one can compare the effect that the carbene and the aldehyde have on the ring proton that is closest to it. The signal of H3 is shifted downfield more than H3 of **1**. The aldehyde functionality also draws electron density out of the ring and competes with the carbene functionality.

Complex **14**, having no ring hydrogen atoms, displays the characteristic aldehyde signal around 10 ppm and also the ethoxy substituent's signals at 4.36 and 1.51 ppm. These signals fall almost at the same locations as the equivalent signals of **3**. It means that the aldehyde does not greatly affect the ethoxy substituent in terms of proton shielding/deshielding.

---

[3] Patent – see website: http://www.wipo.int/pctdb/en/wo.jsp?IA=CA2005000131&DISPLAY=DESC
[4] G.–M Xia, P. Lu, G–B. Xu; *J. Serb. Chem. Soc.*, **2004**, *69*, 335–341

3.1.6 Acyl–hydroxycarbene complexes

In the unique complexes **15** and **16** a hydroxycarbene was trapped in a dinuclear acyl–hydroxycarbene complex. The compounds also display a bridging rhenium–hydride.

The ^{1}H NMR spectrum of **15** is shown in Figure 3.10. Important signals in the spectrum are the high–field and low–field signals that correspond to the two bridging hydrogen atoms of the complex. The peak at 21.5 ppm was assigned to the protonic hydrogen atom that bridges the two oxygen atoms. This hydrogen atom is much deshielded by the oxygen atoms. The singlet at –15.69 ppm was assigned to the bridging hydride hydrogen atom that bridges the two rhenium atoms and is shielded by the rhenium atoms.

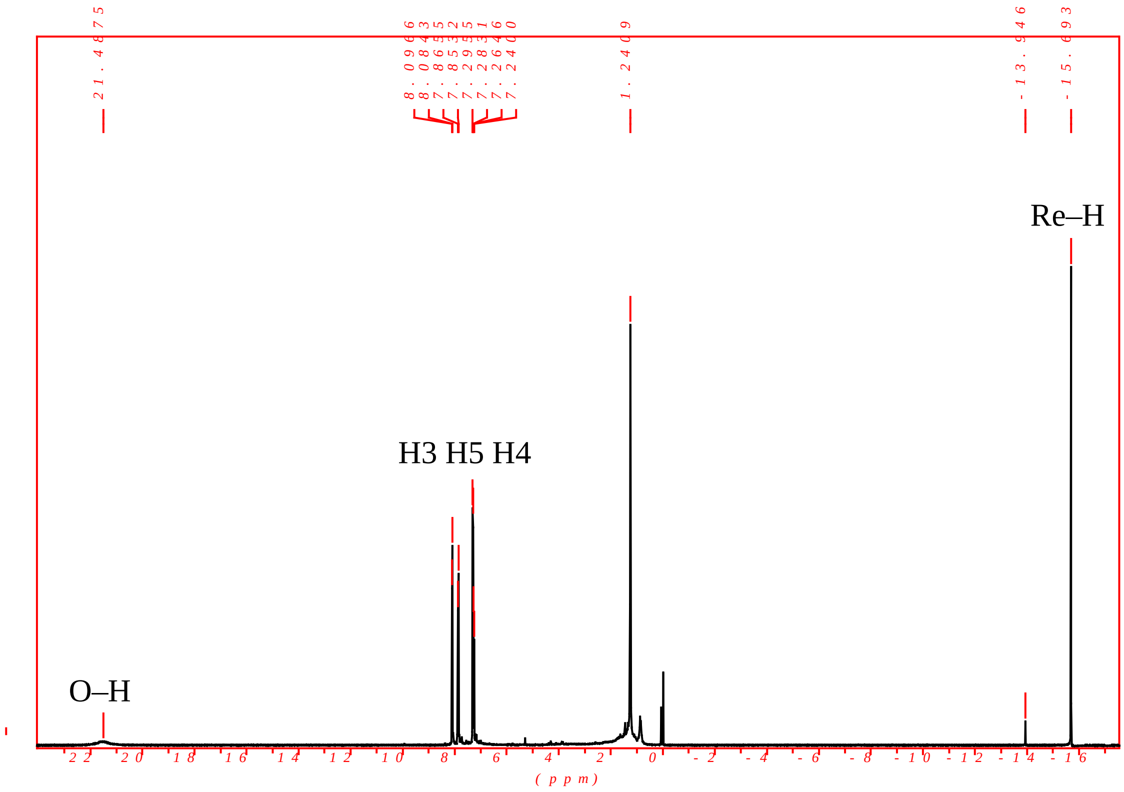

Figure 3.10: ^{1}H NMR spectrum of **15** in $CDCl_3$

A small hydride signal at –13.95 ppm has not been assigned. It is possible that the complex dissociates in solution to another hydride complex[5]. Proton NMR data is given in Table 3.6.

Table 3.6: ^{1}H NMR data (δ, J (Hz), $CDCl_3$) for **15–16**

Complexes:	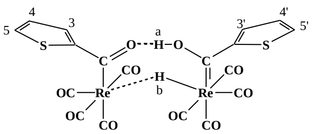 **15**	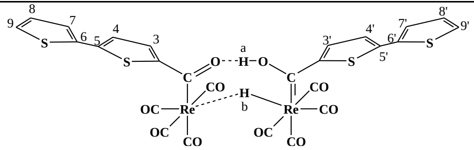 **16**
H3	8.09 (d, 3.0)	8.01 (d, 3.8)
H4	7.28 (dd, 3.0; 1.5)	7.49 (d, 3.8)
H5	7.86 (d, 1.5)	–
H7	–	7.18 (d, 4.5)
H8	–	7.05 (t, 4.5)
H9	–	7.72 (d, 4.4)
Ha	21.5 (br)	21.3 (br)
Hb	–15.7 (s)	–15.7 (s)

It is interesting that corresponding hydrogen atoms on the two thiophene rings (**15**) and the bithiophene rings (**16**) are equivalent (their signals coincide). This shows that at room temperature in solution the complexes are symmetrical, and the two constituent parts lose their individual identity. Since peaks are not broadened one could also assume that the complexes are rigid. The inflexibility is believed to come from the framework created by the O–H–O and Re–H–Re bonds. Also, the extended double bond character, between the rhenium atoms and the carbene carbon atoms and the carbene carbon atoms and the oxygen atoms, may contribute to rigidity. For complex **15** the following two resonance structures can be drawn which changes the one fragment into the other (Scheme 3.4). The same is held to be true and applicable for **16**.

---

[5] C. S. Yang, C. P. Cheng, L. W. Guo, Y. Wang; *J. Chin. Chem. Soc.*, **1985**, *22*, 17–22

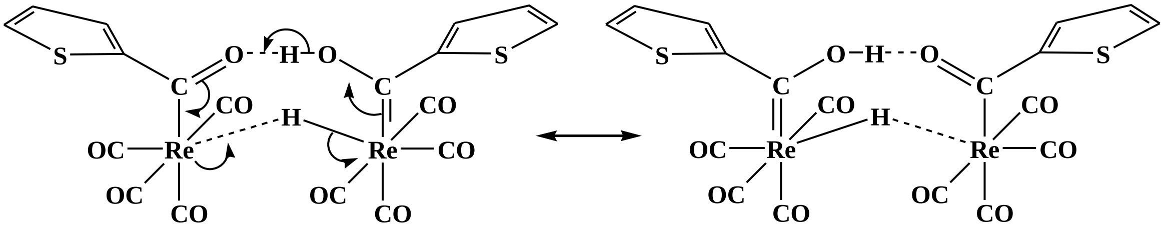

Scheme 3.4: Resonance forms of **15**

A high–field hydride signal is a positive indication of these complexes. For most monorhenium complexes the hydride signal is seen in the range –4 to –10 ppm and for the dirhenium complexes with a bridging hydride, its signal is commonly seen in the range of about –14 to –20 ppm[6]. The protonic hydrogen NMR signals can appear over a large range. In the Shvo catalyst[7], the signal of the bridging protonic hydrogen atom is at 8 ppm, versus signals around 21 ppm for **15** and **16**. The signal of the bridging hydride in the Shvo complex appears at –17.91 ppm, which is closer to the observed proton NMR spectroscopy values of the two complexes' hydride atoms.

A comparison of ^{1}H NMR signals of the thiophene substituents of **15**, with the equivalent thiophene signals of the thiophene monocarbene complexes **1** and **7**, would indicate that the double bond delocalization towards the carbene (acyl) carbon is most effective for **15**. The H3 signal at 8.09 ppm is at lowest field strength and the same goes for the other two ring protons, H4 and H5. The same can however not be said for **16**. For instance, the H3 signal of the monorhenium bithiophene complex **5** is at lowest field strength, lower than the H3 signal of **16**.

---

[6] Re(Cp) complexes: (a) C. P. Casey, C. J. Czerwinski, R. K. Hayashi; *J. Am. Chem. Soc.*, **1995**, *117*, 4189–4190; (b) J. R. Krumper, R. L. Martin, P. J. Hay, C. M. Yung, J. Veltheer, R. G. Bergman; *J. Am. Chem. Soc.*, **2004**, *126*, 14804–14815
Dirhenium complexes with bridging hydrogen atom: (c) R. D. Adams, B. Captain, C. B. Hollandsworth, M. Johansson, J. L. Smith, Jr.; *Organometallics*, **2006**, *25*, 3848–3855
Clusters: (d) R. D. Adams, O.–S. Kwon, J. L. Perrin; *J. Organomet. Chem.*, **2000**, *596*, 102–108

[7] Y. Shvo, D. Czarkie, Y. Rahamim; *J. Am. Chem. Soc.*, **1986**, *108*, 7400–7402

3.2. Carbon NMR spectroscopy data

The carbene carbon NMR resonance of rhenium Fischer carbene complexes can appear over a large range of chemical shift values and they reflect the electrophilic nature of the carbene carbon. In Table 3.7, some carbene carbon NMR data from literature is given, values that appear in the same range as those of the carbene carbon atoms of the prepared complexes.

Table 3.7: ^{13}C NMR chemical shifts for monocarbene complexes of rhenium, [ReL$_5$(carbene)]$^{n+}$ (n = 0, 1)

Re Ligands	Carbene substituents	Carbene carbon resonance (ppm)	Ref.
Triphos 2xCO	–OCH$_3$; –1–CH$_2$–(1,2–hexene)	307.8 (CDCl$_3$)	8
Cp 2xCO	–OCH$_3$ –CH$_3$	289.5 (C$_6$D$_6$)	9
Triphos 2xCO	–OH; –C(H)=C(H)(C$_6$H$_5$)	282.7 (CD$_2$Cl$_2$)	5
Cp 2xCO	–OCH$_3$ –Cp(Re(CO)$_3$);	271.2 (CD$_2$Cl$_2$)	10

3.2.1 Monocarbene dirhenium nonacarbonyl complexes

In the ^{13}C NMR spectrum of complex **1** the carbene carbon signal is observed at 294.8 ppm. Of all the carbon atoms of the complex, its signal falls at lowest field strength, showing significant deshielding of the carbene carbon atom (a Fischer carbene carbon atom is electron–poor). Three signals between 120 and 140 ppm are assigned to thiophene ring carbon atoms C3, C4 and C5. The signal of the *ipso* carbon C2 is at lower

---

[8] C. Bianchini, N. Mantovani, L. Marvelli, M. Peruzzini, R. Rossi, A. Romerosa; *J. Organomet. Chem.*, **2001**, *617–618*, 233–241

[9] K. I. Goldberg, R. G. Bergman; *J. Am. Chem. Soc.*, **1989**, *111*, 1285–1299

[10] C. P. Casey, C. J. Czerwinski, R.K. Hayashi; *Organometallics*, **1996**, *15*, 4362–4365

field strength and of weaker intensity. The carbon NMR shift of the carbonyl ligands of the dirhenium fragment appear as a broad signal around 192.5 ppm. Signals are broadened due to scrambling of carbonyl signals. None of the spectra were recorded at low temperature.

The ^{13}C NMR spectrum of **2** is shown in Figure 3.11. The carbene signal is at higher field strength than that of **1**. There are a greater number of signals in the region of the aromatic rings, corresponding to the substituent in this monocarbene complex being bithiophene and not thiophene and they appear over a larger range: 120 to 160 ppm. Signals between 20 and 32 ppm belong to impurities in the deuterated solvent.

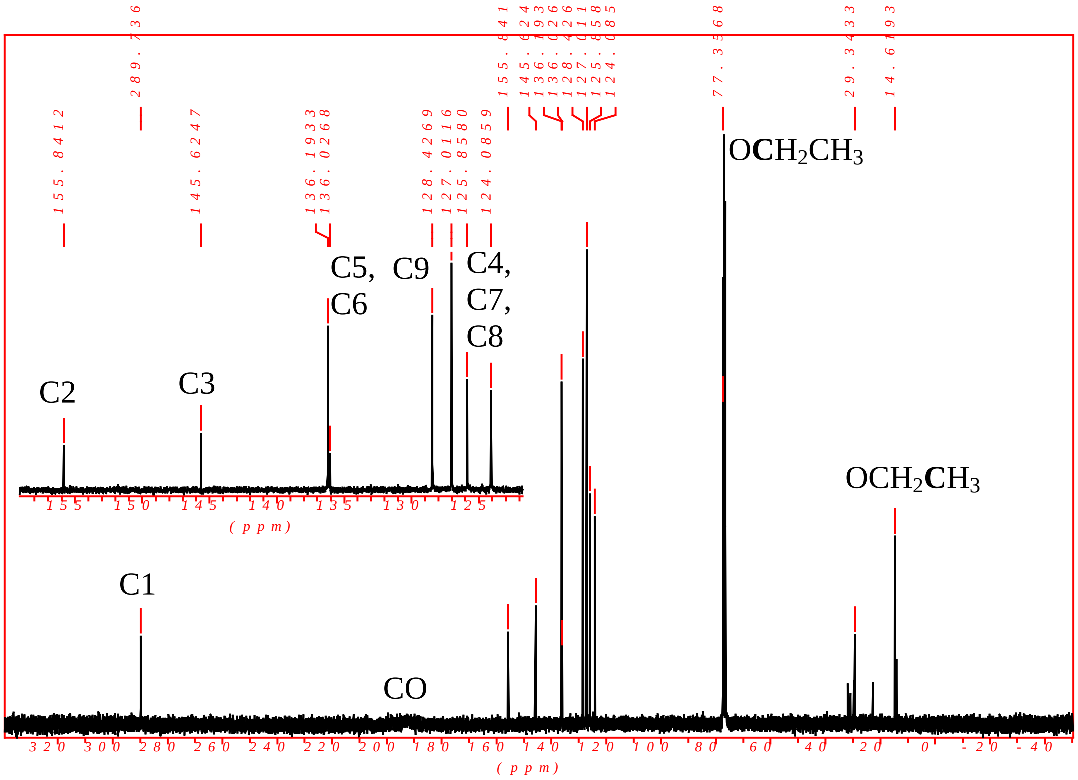

Figure 3.11: ^{13}C NMR spectrum of **2** in $CDCl_3$

The ^{13}C NMR spectral data for the complexes are given in Table 3.8. Again the carbonyl signals are broad because of CO scrambling. These signals are poorly visible for **1** and **3**, but well–defined for **2**.

Table 3.8: ^{13}C NMR spectral data for monocarbene complexes (δ, $CDCl_3$)

Complex	^{13}C NMR bands (ppm)
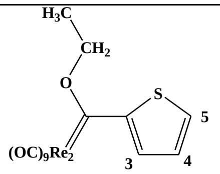 **1**	294.8 (carbene); 192.8 (CO); 157.9 (C2) 132.8 (C3); 132.5 (C5); 127.6 (C4); 77.3 ($\mathrm{O\mathbf{C}H_2CH_3}$); 14.6 ($\mathrm{OCH_2\mathbf{C}H_3}$)
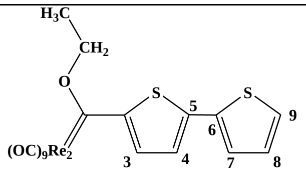 **2**	289.8 (carbene); 198–186 (CO); 158.0 (C2); 145.6 (C3); 136.2 (C5); 136.0 (C6), 128.4 (C9), 127.0, 125.9, 124.1 (C4, C7, C8); 77.4 ($\mathrm{O\mathbf{C}H_2CH_3}$); 14.6 ($\mathrm{OCH_2\mathbf{C}H_3}$)
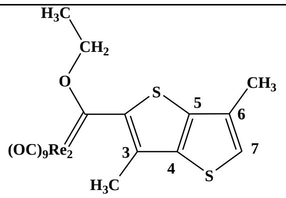 **3**	301.7 (carbene); C2 not observed; CO not assigned; 130.6, 125.0 (ring carbon atoms); 67.0 ($\mathrm{O\mathbf{C}H_2CH_3}$); 31.0, 32.3 (Me3, Me6)

Complex **2**'s carbene carbon signal is at highest field strength. Based on this data, the ethoxy groups of **1** and **2** provide equivalent carbene stabilization (π–donation), but the ethoxy group of **3** provides significantly less stabilization to the carbene carbon of the complex. ^{1}H NMR spectroscopy data (Table 3.1) also shows the ethoxy signals of **3** at slightly higher field, versus the same signals of **1** and **2**.

The signals of the C2 carbon atoms are expected to be shifted downfield significantly (compared to the free thienyl substrates) and that of the other thiophene ring carbon atoms to a lesser extent. This shift for complex **1** is 33.0 ppm downfield and for **2** is 16.6 ppm downfield. The C2 signal of **3** was not observed.

3.2.2 Biscarbene tetrarhenium complexes

Uncleaved biscarbene complexes **7** and **8** could be studied by ^{13}C NMR spectroscopy. Excessive decomposition left ^{13}C NMR spectra of complex **9** useless.

Compared to the ^{13}C NMR spectrum of **2**, the spectrum of **8** (Figure 3.12) is much simpler due to the fact that the complex is symmetrical and equivalent carbon atoms on the two sides are in the same chemical environments. One expects four signals for the ring carbon atoms. As was the case with complex **2**, the signals for the ring carbon atoms of **8** appear over a range from 120 to 160 ppm.

Note that the signal of C2 is not observed in the spectrum given in Figure 3.12, but it was indeed observed on another ^{13}C NMR spectrum measured at a different pulse width. The signals for the other three ring carbon atoms are seen at 143, 135 and 126 ppm.

Unfortunately no signal is seen for the carbonyl ligands of the rhenium metals.

The signals of the ethoxy group carbon atoms are located at 77.7 ($O\mathbf{C}H_2CH_3$) and 14.6 ppm ($OCH_2\mathbf{C}H_3$). The value of the "CH_2" carbon atom is close to the location of the equivalent carbon atom of monocarbene bithiophene complex **2** and the "CH_3" is at the same location as its equivalent in **2**.

Peaks at 29.7 and 1.01 ppm are impurities in the $CDCl_3$.

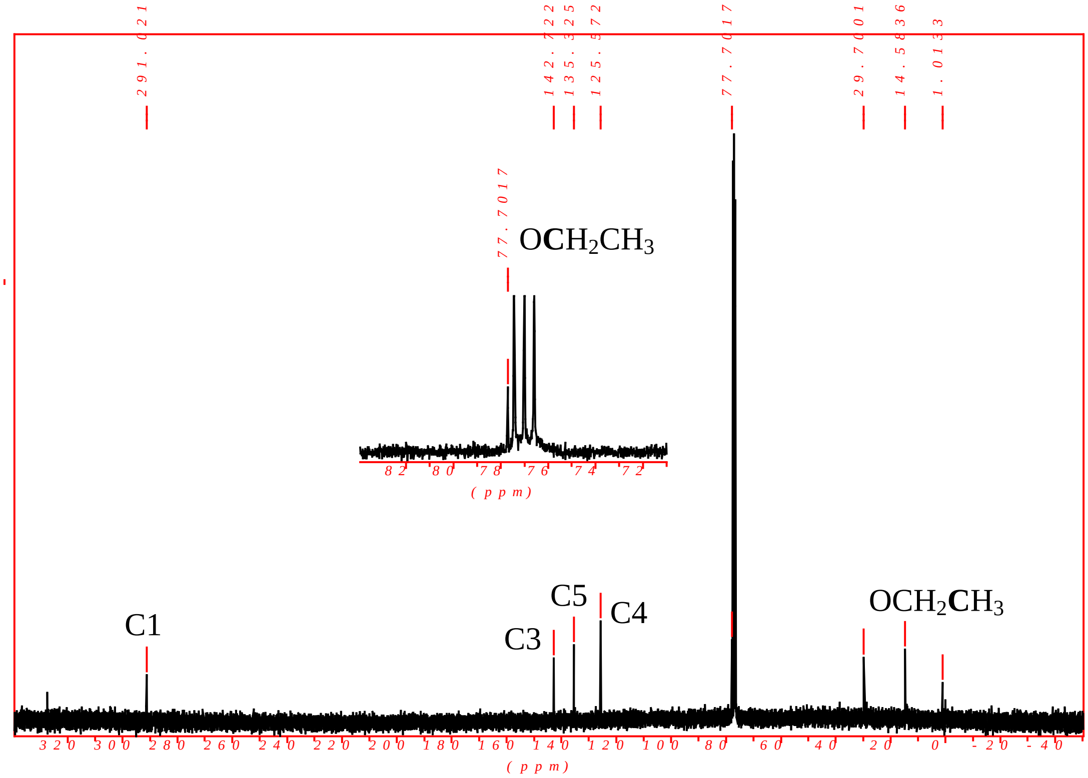

Figure 3.12: ^{13}C NMR spectrum of **8** in $CDCl_3$

The carbene carbon atom signals of the complexes are close to that seen for the carbene carbon atoms of the monocarbene complexes and the same is true for the signals of the ethoxy carbon atoms.

It can be seen that the C2/C2′ signals of the thiophene biscarbene complex are shifted downfield slightly compared to the location of the C2 signal of complex **1**. The C3/C3′ signals are shifted upfield, slightly. Compared to **2**, the signals of C2 and C5 of **8** are about at the same locations. Based on the principle that there is some independence between the two sides of **8**, one side can be approximated to the thiophene monocarbene complex. The values do not have a direct correspondence. The signals at C2 and C4 are found upfield and the signals at C3 and C5 are found downfield compared to the equivalent protons of thiophene monocarbene complex **1**.

Table 3.9: ^{13}C NMR spectral data for biscarbene complexes (δ, CDCl$_3$)

Complex	^{13}C NMR bands (ppm)
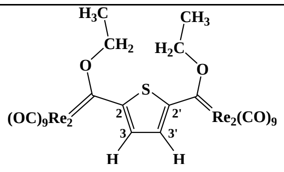 **7**	295.6 (carbene); 193.2 (br, CO); 161.0 (C2, C2′); 130.3 (C3, C3′); 77.5 (O**C**H$_2$CH$_3$); 14.6 (OCH$_2$**C**H$_3$)
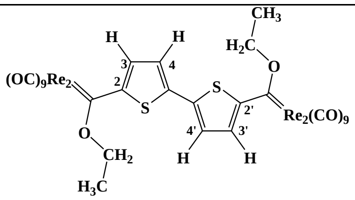 **8**	291.0 (carbene); 155.8 (C2, C2′); 142.7 (C3, C3′); 125.6 (C4, C4′); 135.3 (C5, C5′); 77.7 (O**C**H$_2$CH$_3$); 14.6 (OCH$_2$**C**H$_3$)

3.2.3 Cleaved monocarbene complexes

The ^{13}C NMR spectroscopy data of the three complexes are given in Table 3.10.

Compared to their locations in the uncleaved complexes **1**–**3**, the signals of the carbene carbon atoms are shifted upfield and not downfield. The following values reflect it:
Complex **4**: 294.8 to 260.4 ppm (–34.4 ppm)
Complex **5**: 289.8 to 268.0 ppm (–21.8 ppm)
Complex **6**: 301.7 to 272.1 ppm (–29.6 ppm)

The carbene carbon ^{13}C NMR signals of the three complexes appear within a range of about 12 ppm, with the thiophene complex's carbene carbon being most shielded and the 3,6–dimethylthieno[3,2–*b*]thiophene complex's carbene carbon being least shielded. It is possible that the pendant methyl group at location 3 of complex **9**'s thienyl substituent may prevent coplanarity between the aromatic substituent and the ring and thus reduce electron delocalization from the R–group into the empty carbene p–orbital.

Table 3.10: ^{13}C NMR data for monocarbene complexes (δ, $CDCl_3$)

Complex	^{13}C NMR bands (ppm)
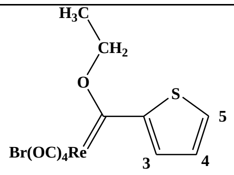 **4**	260.4 (carbene); CO not observed; 137.3 (C2); 134.7 (C3); 128.5 (C4); 138.3 (C5); 77.2 (OCH_2CH_3); 14.5 (OCH_2CH_3)
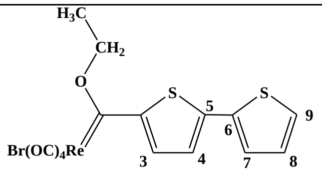 **5**	268.0 (carbene); 192 (CO); 152.8 (C2); 135.7 (C5); 148.6 (C3); 131.8 (C6); 129.0 (C9); 128.8, 127.6 (C4, C7); 125.7 (C8); 78.8 (OCH_2CH_3); 15.1 (OCH_2CH_3)
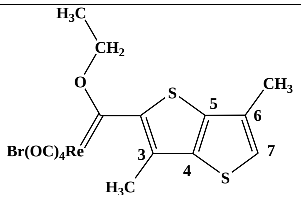 **6**	272.1 (carbene); 186.0; 184.3 (CO); 151.0 (C2); 146, 151.0 (C4, C5); 137.2 (C3); 131.2 (C6, C7); 31.6, 32.0 (Me3, Me6) 79.7 (OCH_2CH_3); 15.7 (OCH_2CH_3);

The value of C2 of thiophene (**4**) differs a lot from that of C2 in the other two complexes – it appears at much higher field strength. The ethoxy groups' carbon signals are roughly the same, so the extra density (for carbene stabilization) has to come from the metal. If the metal donates more electron density to the carbene carbon, there is less electron–density left on the metal to donate to the carbonyl ligands.

3.2.4 Complex 15 and 16

The ^{13}C NMR spectrum of **15** is given below in Figure 3.13. The signals of the carbene carbon, the carbonyl ligands and the thiophene carbon atoms are all observed. There are some small unidentified peaks in the spectrum, which may belong to a dissociation product. It is also possible that, in solution, this complex breaks up into a 16–electron and the 18–electron complex and that one sees signals for these two different fragment complexes.

The carbene carbon signal at 260.3 ppm lies at about the same location in the spectrum as do the carbene carbon signal of **7**, showing that these two carbon atoms are similarly shielded. The carbene carbon atom of this complex is presumed to have some acyl character and there is expected to be a degree of double bonding between it and the oxygen atom.

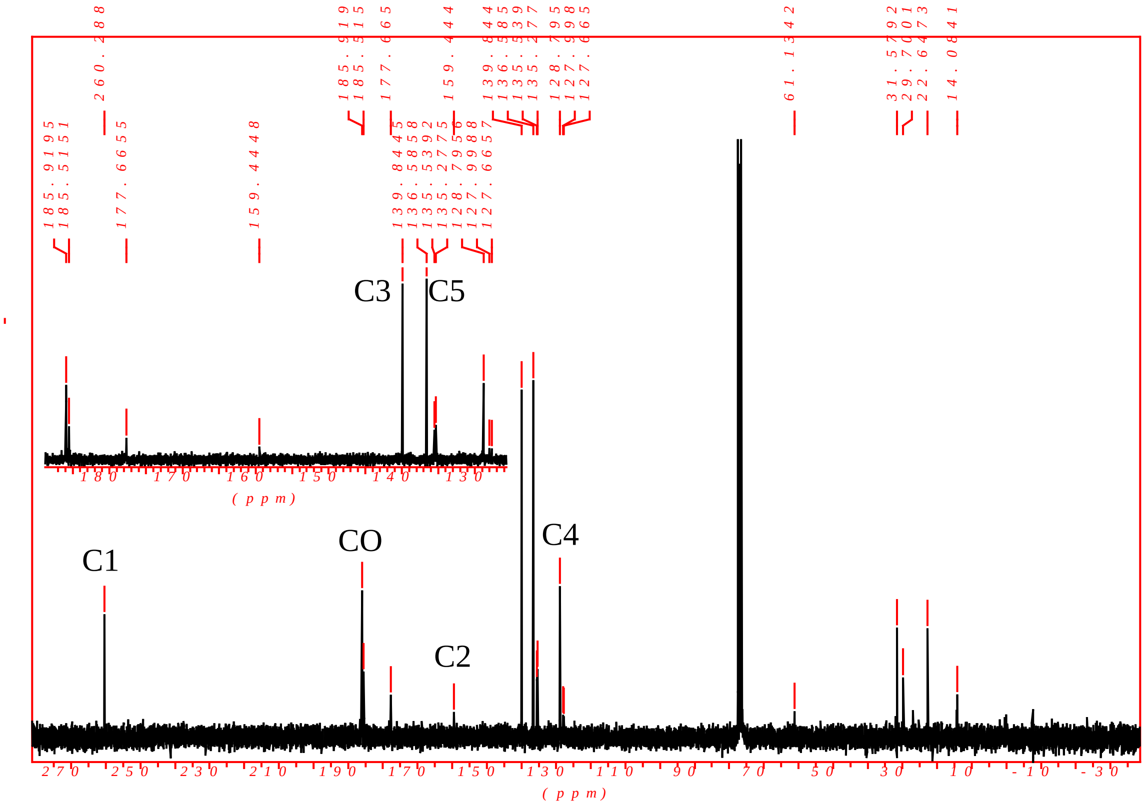

Figure 3.13: ^{13}C NMR spectrum of **15** in $CDCl_3$

In the spectrum there are three signals that might be assigned to the carbonyl carbon atoms. They are well–resolved and located at 185.9, 185.5 and 177.7 ppm. It is presumed that the last would belong to the carbonyl carbon atom that is *trans* to the carbene (acyl) ligand or trans to the hydride ligand. The signal at 185.5 ppm likely belongs to the two equivalent equatorial carbonyl ligands that are cis to the carbene (acyl) ligand.

Table 3.11: ^{13}C NMR spectral data for **15** and **16**

Complex	^{13}C NMR bands (ppm)
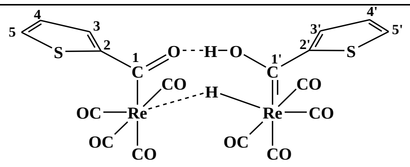	260.3 (carbene); 185.9, 185.5, 177.7 (CO); 159.5 (C2); 139.8 (C3); 128.8 (C4); 136.6 (C5)
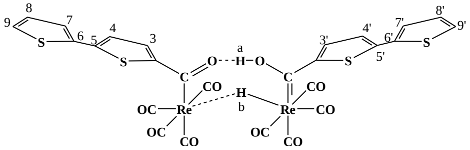	259.0 (carbene); 193 (br, CO); 152.5 (C2); 141.1, 134.9, 126.5, 125.9, 124.0 (C3, C4, C7, C8, C9); C5, C6 not observed.

As was also observed with proton NMR spectroscopy, the two sides of the molecule (equivalent carbon atoms) give coinciding signals in the ^{13}C NMR spectrum. The carbene/acyl–carbon atom signal is shifted upfield significantly for **15** and **16** from the carbene carbon atom of **1** and **2**, respectively, which we ascribe to greater acyl character. Electron delocalization over the 8–membered ring is shown in Figure 3.14.

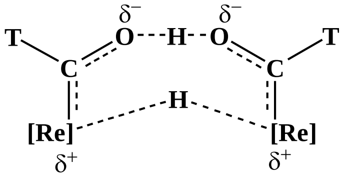

Figure 3.14: Electron delocalization in complexes **15** and **16** over the cyclic 8–membered ring

3.3 IR spectroscopy data

The vibrational spectra of all the complexes were determined in hexane by infrared spectroscopy. The carbonyl region of the spectra was studied. In Figure 3.15, the infrared spectra of complexes **2**, **5** and **15** are shown. The infrared spectrum of **5** also contains signals of [Re(CO)$_5$Br] (2100, 2045 cm^{-1}), the other product of Re–Re bond cleaving.

The infrared spectrum of **15** was examined and no acyl signal was observed in the acyl region.

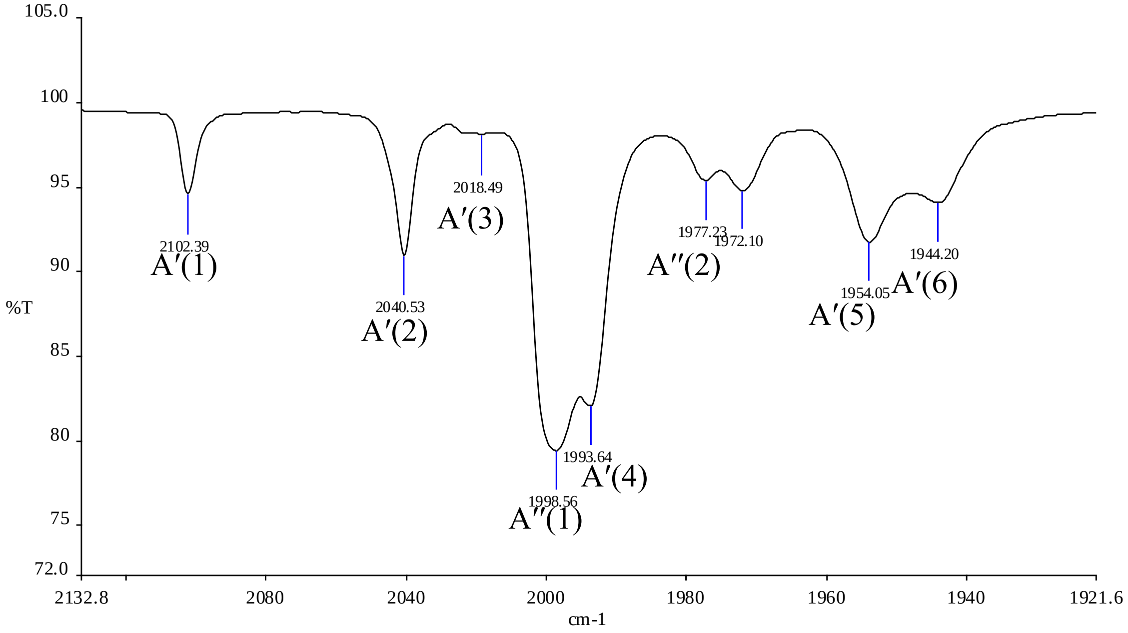

Complex **2**

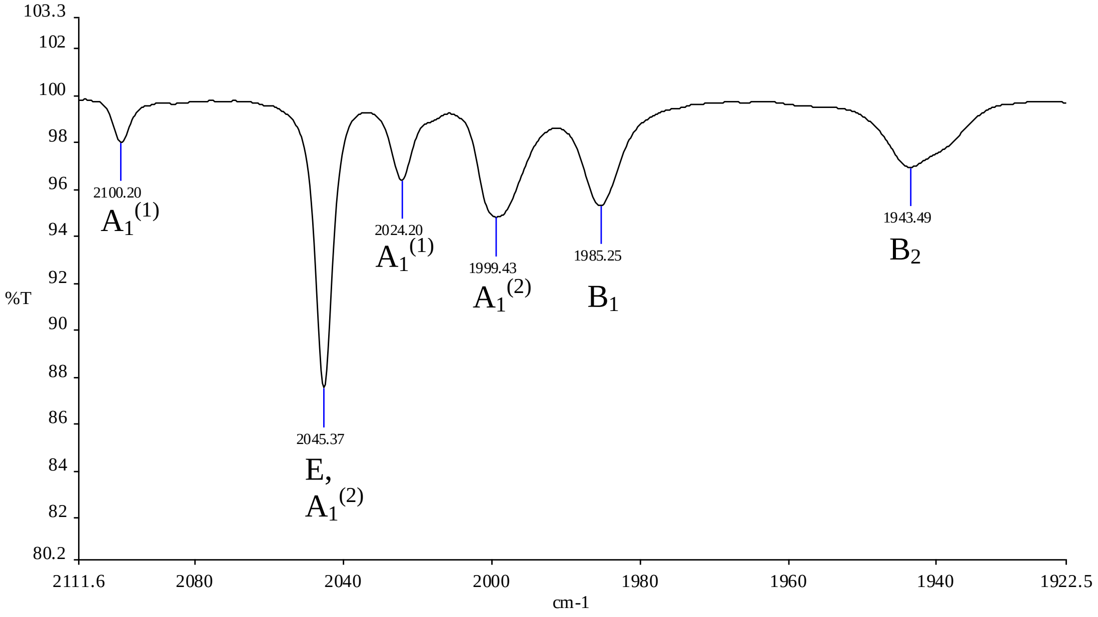

Complex **5**

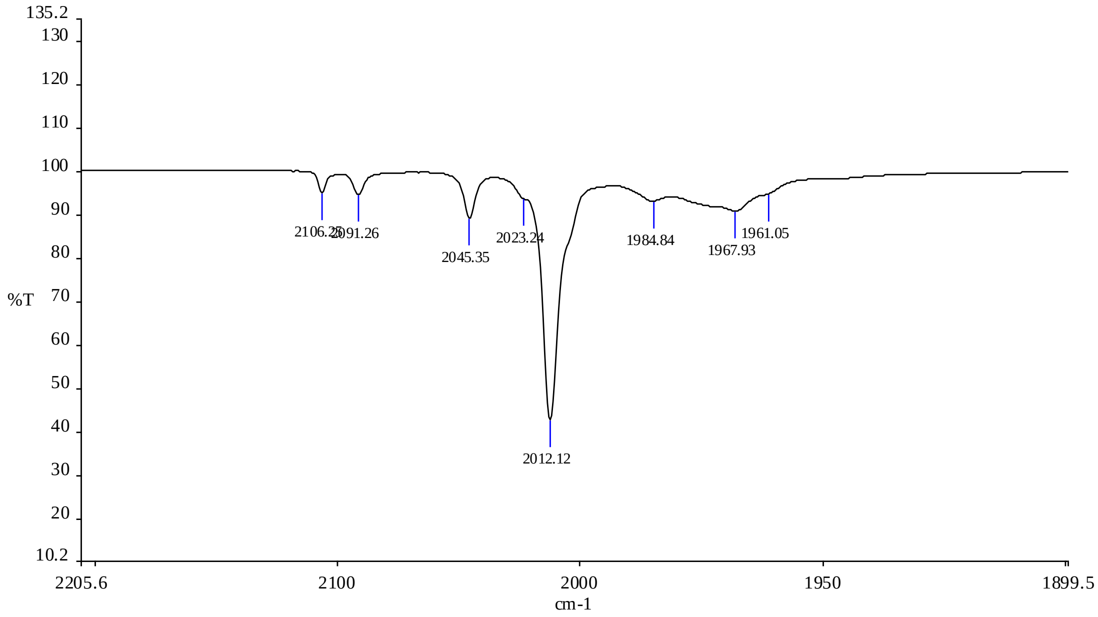

Complex **15**

Figure 3.15: IR spectra (ν_{CO}–region, cm^{-1}) of complexes **2**, **5** and **15**

Infrared spectroscopy was used to primarily determine whether the complex was a monorhenium monocarbene carbonyl complex, *cis*–Re(CO)$_4$ ($C_{2\upsilon}$), or a dirhenium monocarbene complex, *eq*–Re$_2$(CO)$_9$ (C_s). One can also deduce from the pattern of bands whether the complex is a monocarbene or a biscarbene (or even more carbene ligands) dirhenium complex.

In all cases it was found that there is only one carbene ligand per dirhenium or rhenium unit. Infrared spectroscopy confirmed this, as well as giving information of the specific stereoisomer of the complex. The IR spectroscopy data of the complexes are given in Tables 3.12, 3.13 and 3.14.

The complexes in Table 3.12 have equatorial carbene ligands of dirhenium nonacarbonyl units. One finds C_s symmetry and 9 infrared signals for these types of complexes, Figure 3.16. An axial dirhenium nonacarbonyl complex ($C_{4\upsilon}$) will display five bands.

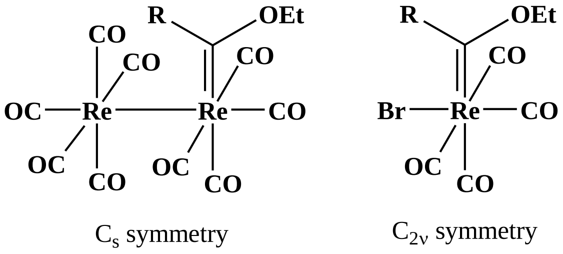

Figure 3.16: Symmetry of monocarbene complexes

Comparing the spectra of the uncleaved complexes with that of the cleaved complexes, one clearly sees the difference between a dirhenium 9–carbonyl complex and a single metal four–carbonyl complex. There are only 4 signals in the infrared spectrum of the cleaved Re–bromide carbene complexes.

Table 3.12: IR spectroscopy data (ν_{CO}–region, cm^{-1}) of uncleaved complexes

Complex	Structure	Bands[a] (cm^{-1})
1	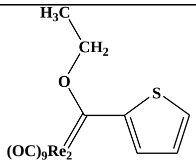	2103 (w); 2071 (w); 2042 (m); 2015 (vs); 2002 (s); 1994 (s); 1977 (s); 1955 (m); 1945 (w)
2	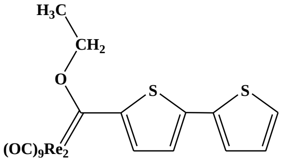	2102 (w); 2041 (m); 2018 (s); 1999 (vs); 1994 (vs); 1977 (w); 1972 (w); 1954 (m); 1944 (w)
8	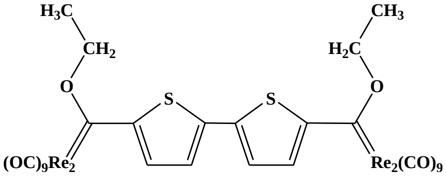	2102 (w); 2045 (s); 2029 (m); 2012 (w); 2001 (vs); 1994 (vs); 1983 (m); 1954 (m)

[a] Signals can range from very weak to very strong and it is indicated by: vw = very weak; w = weak; m = medium; s = strong; vs = very strong.

Table 3.13: IR spectroscopy data of cleaved carbene complexes (carbonyl region)

Complex	Structure	Bands (cm^{-1})
4	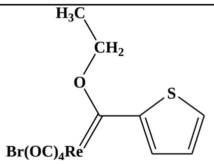	2071 (s); 2015 (s); 2004 (s); 1977 (s)
5	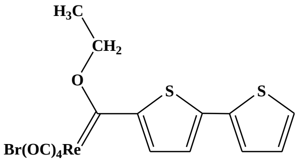	2024 (m); 1999 (s); 1985 (s); 1943 (m)
6	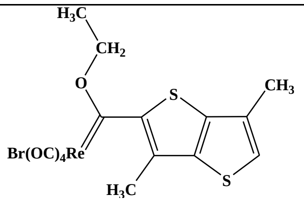	2046 (s); 1999 (vs); 1985 (m); 1947 (w)

The carbonyl stretching frequencies of **4** are at significantly higher wavenumbers than those of the other two monocarbene complexes. This is in agreement with the NMR data of the thiophene monocarbene complex versus the other two monocarbene complexes. Less back–bonding to CO ligands means stronger C–O bonds and higher wavenumbers.

Table 3.14: Infrared spectrum of complex **15** (carbonyl region)

Complex	Structure	Bands (cm^{-1})
15	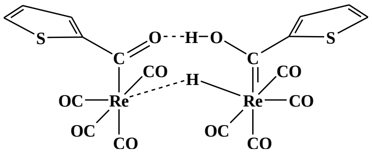	2106 (w); 2091 (w); 2045 (m); 2023 (w); 2012 (vs); 1985 (w); 1968 (w); 1961 (w)

It seems puzzling that complex **15** should have so many carbonyl bands in the infrared spectrum. As each rhenium atom has four CO ligands one would expect a CO band pattern that is similar to other O_h complexes with four CO ligands and one would also expect that the carbonyl ligands on the two metal fragments should give coinciding infrared signals, as was the case with the NMR data. Seemingly the two fragments' CO ligands absorb at different wavelengths and signals are duplicated. Infrared and NMR spectroscopy have very different time–domains, with the former being faster than the latter by a factor of about 10^{10}. This would suggest that the species are quickly interconverting and this is observed with IR spectroscopy, where NMR spectroscopy only shows a time–averaged structure.

There is the possibility that the complex dissociates in solution into its two fragments. The signal of the carbene–oxygen may also appear in this area, as it was not observed in the typical region where one observes acyl ligand C–O vibrational absorptions.

3.4. Mass spectrometry data

3.4.1 Complex 1

A part of the mass spectrum of **1** is shown in Figure 3.17 (showing the M^+ peaks) and the whole spectrum in Figure 3.19. The fragmentation data of complex **1** is given in Table 3.15.

Rhenium occurs in nature in two isotopic forms: ^{185}Re (37%) and ^{187}Re (63%). In the mass spectrum, one observes peak groupings and these correspond to specific molecular ions. The M^+ molecular ion peak is observed at *m/z* = 763.6/765.6 (two values for two rhenium isotopes).

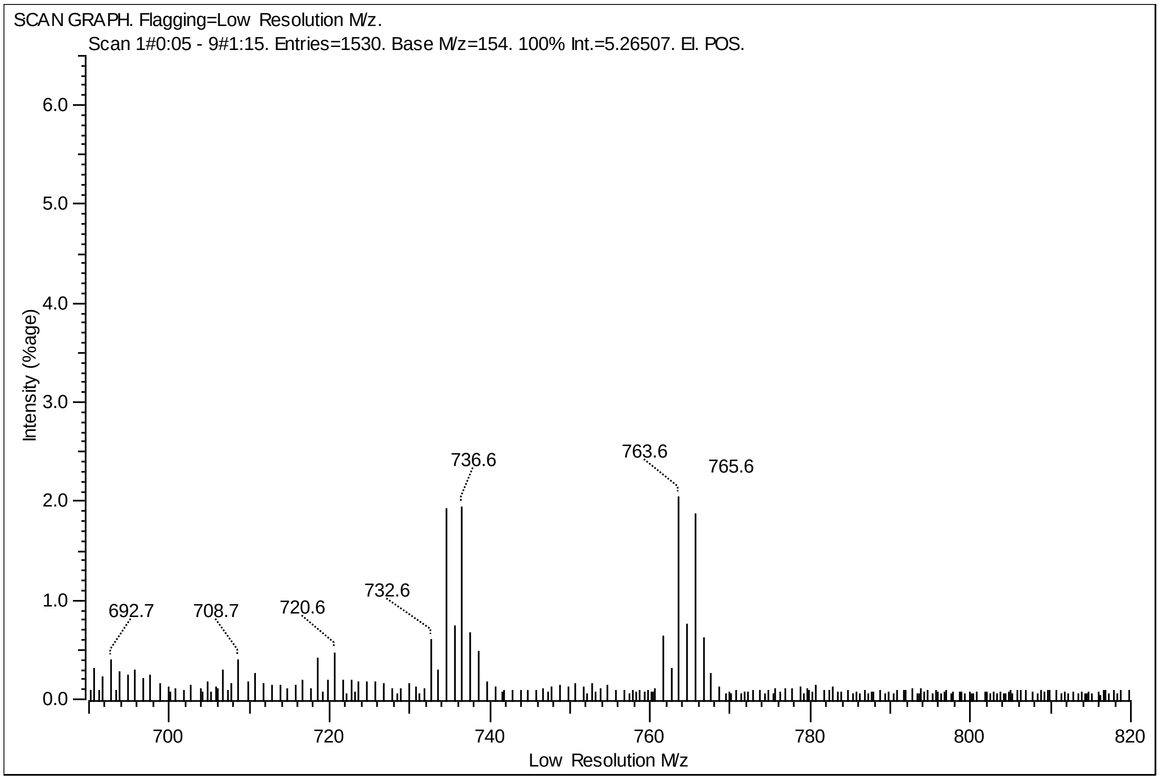

Figure 3.17: Part of the mass spectrum of **1**

It can be seen on Figure 3.19 that the peaks in the range from 500 to 800 *m/z* are all small peaks. This would indicate a rapid loss of all carbonyl ligands. The first strong peak is at *m/z* = 439.8 (68%), which corresponds to the M^+–$Re(CO)_5$ ion. The peak at *m/z* = 327, which represents $Re(CO)_5{}^+$, is much weaker, indicating fragmentation pathways that show an initial rhenium–rhenium bond cleavage as well as the elimination of carbonyl ligands. The principle ion is at *m/z* = 154. This corresponds to an unknown molecular ion without Re. There are also peaks at *m/z* = 273, 289 and 307 that seem to belong to species without a Re atom (only single peaks). They are difficult to identify.

Assignment of fragment ions are unsubstantiated and more than one fragment ion is possible for a given *m/z* value. For example, the carbene ligand may fragment in various ways giving fragments corresponding to 28 or multiples thereof, see Figure 3.18.

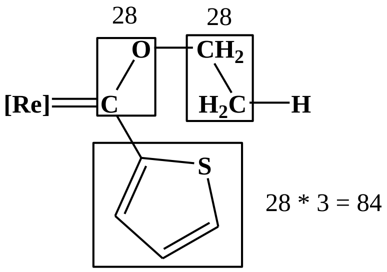

Figure 3.18: Fragments of carbene ligand that displays *m/z* = 28 units

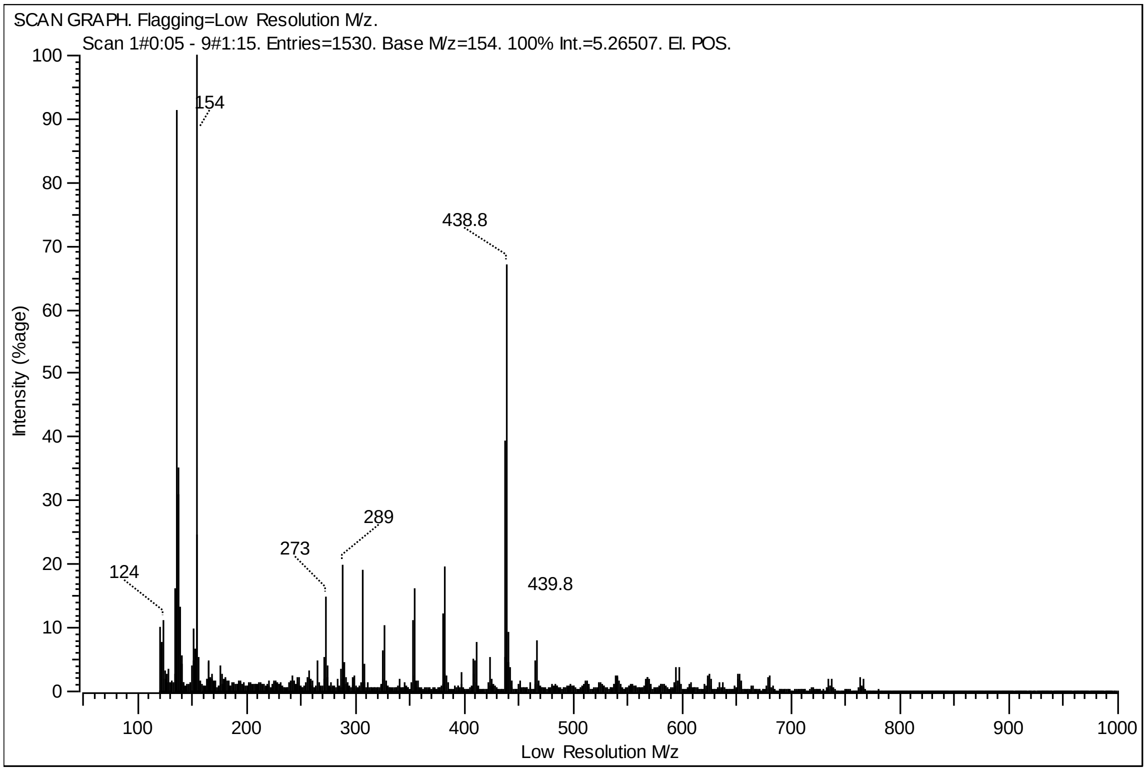

Figure 3.19: Mass spectrum of **1**

Table 3.15: Fragmentation data of **1**

<table>
<tr><td colspan="3">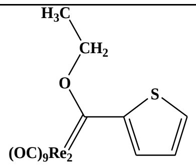 </td></tr>
<tr><td><i>m/z</i></td><td>Intensity (%)</td><td>Molecular ion</td></tr>
<tr><td>763.6; 765.6</td><td>2.1</td><td>M^+</td></tr>
<tr><td>734.6; 736.6</td><td>2.0</td><td>$M^+ – CH_2CH_3$</td></tr>
<tr><td>678.7; 680.7</td><td>2.4</td><td>$M^+ – CH_2CH_3 – 2CO$</td></tr>
<tr><td>650.7; 652.7</td><td>2.8</td><td>$M^+ – CH_2CH_3 – 3CO$</td></tr>
<tr><td>622.7; 624.7</td><td>2.7</td><td>$M^+ – CH_2CH_3 – 4CO$</td></tr>
<tr><td>594.7; 596.7</td><td>3.7</td><td>$M^+ – CH_2CH_3 – 5CO$</td></tr>
<tr><td>567.8; 568.8</td><td>2.2</td><td>$M^+ – CH_2CH_3 – 6CO$</td></tr>
<tr><td>538.8; 540.8</td><td>2.5</td><td>$M^+ – CH_2CH_3 – 7CO$</td></tr>
<tr><td>510.8; 512.8</td><td>1.7</td><td>$M^+ – CH_2CH_3 – 8CO$</td></tr>
<tr><td>464.8; 466.8</td><td>8.5</td><td>$[Re(CO)_5\{C(OEt)C_4H_3S\}]^+$</td></tr>
<tr><td>436.8; 438.8</td><td>68</td><td>$M^+ – Re(CO)_5$</td></tr>
<tr><td>354.8; 355.8</td><td>16</td><td>$[Re(CO)_6]^+$</td></tr>
<tr><td>326.8; 327.8</td><td>11</td><td>$[Re(CO)_5]^+$</td></tr>
</table>

3.4.2 Complex 2

The molecular ion, *m/z* = 845.4 (M^+), was observed for complex **2**. The first peak of high intensity one finds at *m/z* = 548.6. Again this ion represents the fragment ion M^+–$Re(CO)_5$ which emphasized the weakness of the Re–Re bond. In both cases a fragment ion, corresponding to the uptake of a carbonyl i.e. $Re(CO)_6^+$ and $Re(CO)_5$(carbene)$^+$, is observed. Fragmentation data of the complex is given in Table 3.16.

The higher *m/z* values of the mass spectrum of this complex, also features a lot of peaks of low intensity, similar to the spectrum of **1**. This would suggest the rapid loss of CH_2CH_3 and carbonyl ligands.

Table 3.16: Fragmentation data of **2**

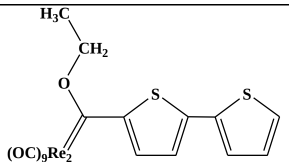		
m/z	Intensity (%)	Molecular ion
845.4; 847.4	2.5	M^+
816.4; 818.3	2.3	$M^+ - CH_2CH_3$
760.4; 762.4	2.0	$M^+ - CH_2CH_3 - 2CO$
732.4; 734.4	2.0	$M^+ - CH_2CH_3 - 3CO$
704.5; 706.5	2.6	$M^+ - CH_2CH_3 - 4CO$
676.5; 678.5	1.9	$M^+ - CH_2CH_3 - 5CO$
648.5; 650.5	2.2	$M^+ - CH_2CH_3 - 6CO$
620.6; 622.6	3.0	$M^+ - CH_2CH_3 - 7CO$
546.6; 548.6	38	$[Re(CO)_5\{C(OEt)C_8H_5S\}]^+$
518.6; 520.6	85	$M^+ - Re(CO)_5$ or $[Re(CO)_4\{C(OEt)C_8H_5S\}]^+$
353.8; 355.8	7	$Re(CO)_6^+$
325.8; 327.8	8	$Re(CO)_5^+$

3.4.3 Complex 3

The M^+ peak (*m/z* = 848, 846) was observed and is of low intensity, as is also the case for complexes **1** and **2**. The fragmentation data of complex **3** is given in Table 3.17 and a similar pattern of fragmentation than those of complexes **1** and **2** was observed.

The largest peak corresponds to the loss of $Re(CO)_5$ from **3**: 848.4→522.6. There is also evidence for step by step CO loss from the complex, but it seems that the loss of $Re(CO)_5$ is preferred.

Table 3.17: Fragmentation data of complex **3**

<table>
<tr><td colspan="3">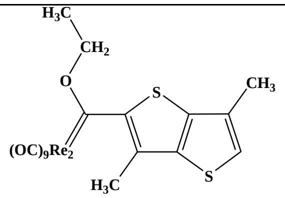
</td></tr>
<tr><td><i>m/z</i></td><td>Intensity (%)</td><td>Molecular ion</td></tr>
<tr><td>848.4; 846.4</td><td>0.6</td><td>M^+</td></tr>
<tr><td>818.3; 820.3</td><td>0.4</td><td>$M^+ – CO$</td></tr>
<tr><td>762.4; 764.4</td><td>1.0</td><td>$M^+ – 3CO$</td></tr>
<tr><td>734.4; 736.4</td><td>1.1</td><td>$M^+ – 4CO$</td></tr>
<tr><td>706.5; 708.5</td><td>1.0</td><td>$M^+ – 5CO$</td></tr>
<tr><td>520.6; 522.6</td><td>62</td><td>$M^+ – Re(CO)_5$/
$[Re(CO)_4\{C(OEt)C_8H_7S_2\}]^+$</td></tr>
<tr><td>492.6; 494.6</td><td>24</td><td>$[Re(CO)_3\{C(OEt)C_8H_7S_2\}]^+$</td></tr>
<tr><td>353; 355</td><td>7</td><td>$Re(CO)_6^+$</td></tr>
</table>

The following scheme represents a summary of the fragmentation observed for the complexes **1**–**3**.

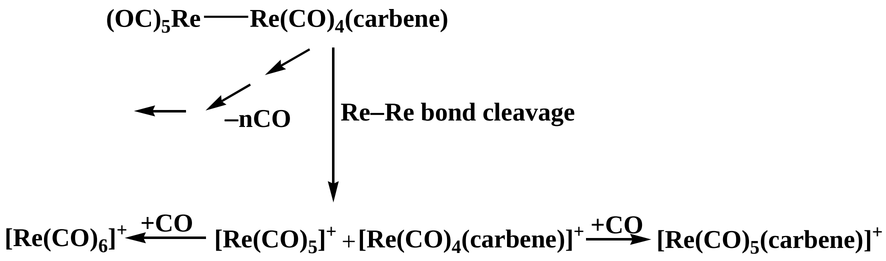

Scheme 3.5: Fragmentation pathway for **1**–**3**

3.4.4 Complexes 8 and 10

No M^+ peak was observed at *m/z* = 1527 (**8**) and 1035 (**10**), respectively. The highest peak observed for **8** is 50 mass units lower at *m/z* = 1477. It is not clear which fragment this represents. There is a signal of high intensity at *m/z* = 959.1, corresponding to the loss of two rhenium atoms and seven carbonyl ligands.

3.4.5 Complex 15

The mass spectrum of **15** is shown in Figure 3.20 and the fragmentation data in Table 3.18. The M^+ is observed at *m/z* = 820.8 and an interesting signal is also seen at the higher value of *m/z* = 959.8. This higher peak shows that the complex combined with another fragment to give a higher–mass molecular cation, but it could not be identified.

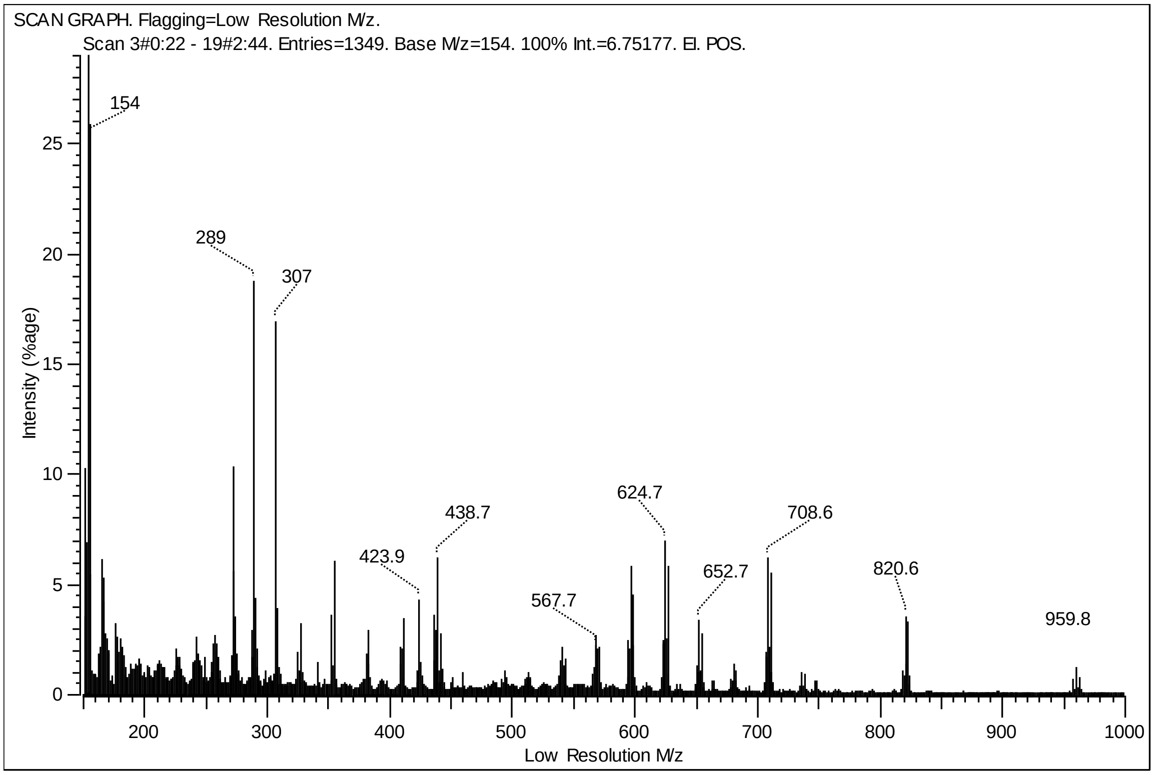

Figure 3.20: Mass spectrum of **15**

It is very insightful that the data shows loss of ten carbonyl groups, where the complex only has eight. This suggests that the CO groups of the acyl/carbene ligands are lost with the other carbonyl ligands.

Table 3.18: Fragmentation data of **15**

<table>
<tr><td colspan="3">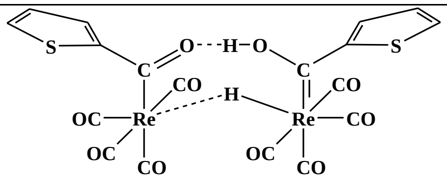 </td></tr>
<tr><td>*m/z*</td><td>Intensity (%)</td><td>Molecular ion</td></tr>
<tr><td>820.6; 822.6</td><td>4.0</td><td>M^+</td></tr>
<tr><td>708.6; 710.6</td><td>6.4</td><td>$M^+ - 4CO$</td></tr>
<tr><td>652.7; 654.7</td><td>3.4</td><td>$M^+ - 6CO$</td></tr>
<tr><td>624.7; 626.7</td><td>7.2</td><td>$M^+ - 7CO$</td></tr>
<tr><td>596.7; 598.7</td><td>6.0</td><td>$M^+ - 8CO$</td></tr>
<tr><td>568.7; 570.7</td><td>3.0</td><td>$M^+ - 9CO$</td></tr>
<tr><td>540.7</td><td>2.1</td><td>$M^+ - 10CO$</td></tr>
</table>